

Effects of PSA and RSA on air bearing slider steady performance

Hong Zhu and David B. Bogy

Computer Mechanics Laboratory
Department of Mechanical Engineering
University of California at Berkeley
Berkeley, CA 94720

ABSTRACT

This report addresses the effects of PSA and RSA on air bearing slider steady performance. We performed simulations for INSIC 7nm, 5nm and 3.5nm FH sliders using the CML static simulator. We found that PSA and RSA have larger effects on steady performance of air bearing slider designs with smaller size and lower FH. We also investigated the effects of suspension stiffness on air bearing slider flying attitude.

1. INTRODUCTION

When using the CML static simulator Quick4 and CML dynamic simulator Dyn4, there are always some differences between the static simulation results and the steady state results of the dynamic simulation. We analyzed the differences and we concluded that the differences were caused by the different default values in the pitch and roll stiffness of the simulators. The two simulators obtained the same results after the input stiffnesses were made the same. From the investigations we did, we also found that the unloaded state of the head-suspension assembly has large effects on air bearing slider performance.

Currently, a zero reference point is assumed for both the CML static and dynamic simulators, which means that pitch torque is zero when the pitch angle is zero and roll torque is zero when the roll angle is zero. With that assumption, the suspension will exert a negative pitch torque on the slider when it is loaded, which consequently causes a lower slider pitch angle and higher FH compared with zero pitch torque case.

In reality, when sliders are mounted to the flexure or gimbal, an initial pitch angle and roll angle result, namely Pitch Static Attitude (PSA) and Roll Static Attitude (RSA). These two angles can greatly affect the magnitude of the pitch and roll torque applied to the slider by the suspension when the slider is loaded onto the disk. In this study, we investigate the effects on PSA and RSA on air bearing slider flying attitude. And we also explore the effects of pitch and roll stiffness on slider steady performance.

2. DEFINITION OF SLIDER SIMULATION PROBLEMS

We consider three different slider designs in this study. [Figures 1 ~ 3](#) show their rail shapes. They are 7nm FH INSIC Pico slider, 5nm FH INSIC Pico slider and 3.5nm FH INSIC Femto slider, respectively. These sliders were designed for the INSIC EHDR projects by using CML optimization programs associated with the CML steady simulator Quick4. Seagate fabricated the 7nm and 5nm FH INSIC Pico sliders and Date Storage Institute fabricated the 3.5nm FH INSIC Femto sliders.

The slider and suspension parameters of these three slider designs are shown in [Table 1](#). We used the pitch stiffness and roll stiffness presented in an example case in the CML Load/Unload User's Manual [\[1\]](#) for all three slider designs. The pitch stiffness is $6.886e-5$ (N-m/rad) and the roll stiffness is $7.049e-5$ (N-m/rad). Therefore we assume that both Pico and Femto sliders were mounted to the same suspension in our study.

3. PSA AND RSA EFFECTS ON SLIDER FLYING ATTITUDE

3.1 Definitions of PSA and RSA

As we mentioned in [Section 1](#), PSA stands for Pitch Static Attitude and RSA stands for Roll Static Attitude. PSA and RSA can be measured once the slider was mounted to the gimbal and they will remain constant thereafter.

[Figure 4](#) shows a typical suspension at unloaded state with positive PSA. And [Fig. 5](#) shows the positive RSA at unloaded state (viewing from slider trailing edge).

[Figure 6](#) shows a typical suspension at loaded state. We see that dimple exerts the normal preload on the center of slider the backside, and the gimbal exerts both pitch torque and roll torque on slider.

3.2 Torques introduced by PSA and RSA

The dependence of pitch and roll torques on PSA and RSA are:

$$\begin{cases} Pitch_Torque = -Pitch_Stiffness \times (Pitch_Angle - PSA) \\ Roll_Torque = -Roll_Stiffness \times (Roll_Angle - RSA) \end{cases} \quad (1)$$

In this study, we modified CML static simulator Quick4 so that it takes pitch stiffness and roll stiffness as input instead of pitch torque and roll torque. We also incorporated PSA and RSA into the code. Therefore, the modified Quick4 can take pitch stiffness, roll stiffness, PSA and RSA as inputs. We used this modification for all the simulations in this study. Also note that, since the intermolecular force has relatively

small effects on the flying attitude of the air bearing sliders considered in this study, we did not include it in the simulations.

3.3 Nominal PSA and RSA values at the unloaded state

In order to define proper PSA and RSA values, we referred to the experimental data for the fabricated 7nm FH INSIC Pico sliders provided by Seagate. [Figures 7](#) and [8](#) show the measured PSA and RSA data for the 87 samples of 7nm FH INSIC Pico sliders, respectively.

We see that PSA ranges from 0.23° to 1.57° . The average PSA is 0.86° with standard deviation 0.31° . RSA ranges from -0.8° to 0.53° . The average RSA is -0.07° with standard deviation 0.24° . Based on those data, we picked up 1° PSA and 0° RSA as our “standard” or “nominal” case.

3.4 PSA effects on air bearing slider steady performance

To investigate the PSA effects on air bearing slider steady performance, we changed the PSA value while keeping the nominal 0° RSA fixed.

Generally speaking, PSA values are positive, as shown in [Fig. 7](#). Negative PSA means a negative initial slider pitch angle, which is bad for slider taking off. So we

consider negative PSA cases as not suitable for a Head-Suspension-Assembly. However, for investigation purposes, we still consider negative PSA cases. In our study, PSA changes between -2° to 2° and it can take the following values: -2° , -1° , -0.75° , -0.5° , -0.25° , 0° , 0.25° , 0.5° , 0.75° , 1° , 2° .

For the 7nm FH INSIC Pico slider the FH, pitch and roll variations with respect to PSA are shown in [Figs. 9 ~ 11](#), respectively. Similarly, [Figs. 15 ~ 17](#) and [Figs. 21 ~ 23](#) show the FH, pitch and roll variations with respect to PSA for the 5nm FH INSIC Pico slider and the 3.5nm FH INSIC Femto slider, respectively. The “Orig.” data in these figures are the steady flying attitude of these three slider designs when assuming 0 pitch torque and 0 roll torque, which is equivalent to 0 pitch stiffness and 0 roll stiffness. The “Orig.” data for those three slider designs are also given in [Table 2](#). Note that we assign zeros to FH, pitch and roll when a slider crashes.

We summarize the above results in [Figs. 27 ~ 29](#).

[Figure 27](#) shows the FH change versus PSA. We see that for all three slider designs, larger PSA causes lower FH. The reason is that, when a slider with PSA is loaded onto the disk, the pitch torque will try to bend the slider pitch angle toward the PSA. Therefore, if the PSA is positive, the pitch torque will increase the pitch angle and thus lower the FH. On the other hand, if the PSA is negative, the pitch torque will lower the pitch angle and thus increase the FH. For the two Pico slider designs the FH change with respect to PSA demonstrates an almost linear dependence, i.e. the FH rate of change

with PSA is nearly constant. So the uniformity of the FHs at the OD, MD and ID almost remains the same. For the 3.5nm FH Femto slider, the FH rate of change is larger, showing that the PSA has larger effects on slider designs with smaller size and lower FH. But we do not observe a linear dependence of FH change versus PSA for the Femto design. With this larger effect of PSA on the FH for the Femto slider design, it is understandable that it crashes onto the disk when the PSA reaches 2° , because a positive PSA always pushes the slider trailing edge towards the disk surface.

Also note that, pitch torque and roll torque still exist even with 0° PSA and 0° RSA. The torques can still be calculated by using formula (1) in this case. Table 3 summarizes the simulation results of these three different slider designs with 0° PSA and 0° RSA. Since the pitch stiffness $6.886e-5$ (N-m/rad) and roll stiffness $7.049e-5$ (N-m/rad) are quite small, the pitch torque and roll torque calculated by using formula (1) are also very small. Therefore, the simulation results with 0° PSA and 0° RSA are very close to the “Orig.” results with 0 pitch torque and 0 roll torque, which are shown in Table 2.

Figure 28 shows the pitch change versus PSA. We see that for all three slider designs, a larger PSA causes higher pitch, as we just analyzed. Furthermore, for all three slider designs, pitch change versus PSA demonstrates a clear linear relationship. The reason for that is the following: since 1° equals $17453.3 \mu\text{rad}$, even 0.25° of PSA, which is $4363.3 \mu\text{rad}$, is overwhelmingly larger than the pitch, which ranges from $100 \sim 300 \mu\text{rad}$ in this study. So we can safely ignore the pitch angle in formula (1) without losing much accuracy and we have:

$$Pitch_Torque \cong Pitch_Stiffness \times PSA \quad (2)$$

This means that for a given suspension, pitch torque is roughly proportional to PSA. This is why it is desirable to include pitch torque as an input parameter in the current CML static simulator. For a slider design, higher pitch torque will increase the slider's pitch and the resulting pitch angle is roughly proportional to the pitch torque exerted on the slider. So we have:

$$Pitch_Torque \cong K \times Pitch_Angle \quad (3)$$

K is a constant for a certain air bearing slider. From [Fig. 28](#) we see that for smaller size Femto slider, K is smaller. From (2) and (3), we have:

$$Pitch_Angle \cong \frac{Pitch_Stiffness}{K} \times PSA = K' \times PSA \quad (4)$$

This is why pitch angle demonstrates a clear linear relationship with PSA. For the two Pico slider designs, since they have similar air bearing surfaces (shown in [Figs. 1](#) and [2](#), respectively) and similar FHs, they have similar constant K'. Therefore their pitch rates of change with respect to PSA are very similar.

In fact, by changing the pitch angle, the air bearing pressure field will change its pattern. For the three air bearing slider designs considered in our study, with higher pitch and lower FH, the pressure at the trailing pad rail will be higher, and the resulting air bearing force will shift toward the slider trailing edge to balance the larger positive pitch torque.

[Figure 29](#) shows the roll change versus PSA. We see that PSA has only small effects on roll angle compared with FH and pitch. With higher pitch angle and lower FH,

we get reduced air bearing force and smaller roll moment caused by the air bearing force, and we get reduced shear force and smaller shear force roll moment. If the roll moment caused by the air bearing force reduces faster than does the roll moment caused by the shear force, the slider will have a slightly higher roll angle so that the roll torque exerted by the suspension can help the air bearing force roll moment balance the shear force roll moment. If the roll moment caused by the shear force reduces faster than roll moment caused by the air bearing force, we will end up with a lower roll angle. From Fig. 29 we see that PSA has larger effects on the roll angles of the Femto slider than it does on the roll angles of the Pico sliders.

3.5 RSA effects on air bearing slider steady performance

Similarly, to investigate the RSA effects on air bearing slider steady performance, we changed the RSA value while keeping the nominal 1° PSA fixed.

Different from PSA, which is usually positive, the RSA can be either positive or negative, as shown in Fig. 8. And it is generally smaller than the PSA. However, for investigation purpose, we still consider large RSA (either positive or negative) cases. In our study, the RSA changes between -2° to 2° and it can take the following values: -2° , -1° , -0.5° , -0.25° , -0.1° , 0° , 0.1° , 0.25° , 0.5° , 1° , 2° .

For the 7nm FH INSIC Pico slider the FH, pitch and roll variations with respect to RSA are shown in Figs. 12 ~ 14, respectively. Similarly, Figs. 18 ~ 20 and Figs. 24 ~ 26

show the FH, pitch and roll variations with respect to RSA for the 5nm FH INSIC Pico slider and the 3.5nm FH INSIC Femto slider, respectively. Again please note that we assign zeros to FH, pitch and roll when the slider crashes.

We summarize the above results in [Figs. 30 ~ 32](#).

[Figure 30](#) shows the FH change versus RSA. We see that, unlike PSA, RSA does not cause a monotonic FH change for the three different slider designs. The reason is that the RSA mainly causes roll angle change and the transducers are located on the central pad rail for all three slider designs considered in our study. Some slider designs install the transducer on the trailing edge of their outer rails. Since positive RSA causes positive roll torque, and positive roll torque causes higher roll angle, and higher roll angle means lower spacing at outer rail according to the IDEMA standards, so we can expect a monotonic FH decrease with higher RSA for those kind of slider designs.

We can also see from [Fig. 30](#) that the RSA has greater effects on lower FH slider designs. The 7nm FH Pico slider flies when RSA changes from -2° to 2° . However the 5nm FH Pico slider crashes when the RSA equals 2° . And the 3.5nm FH Femto slider can only fly with the RSA ranging from -0.25° to 0.25° .

[Figure 31](#) shows the pitch change versus RSA. We see that for all three slider designs, the pitch angle almost remains the same even with large RSA. This shows that RSA has little effect on pitch angles when the PSA is fixed.

Figure 32 shows the roll change versus RSA. We see that larger RSA causes higher roll angles. The reason for this is that, when a slider with a RSA is loaded onto the disk, the roll torque tends to bend the slider roll angle toward the RSA. Therefore, if the RSA is positive the roll torque will increase the roll angle. Similarly, if the RSA is negative, the roll torque will lower the roll angle.

We also see from Fig. 32 that, for all three slider designs, roll change versus RSA also demonstrates a clear linear relationship. The reason for that is the following: Even 0.1° RSA, which is $1745.3 \mu\text{rad}$, is much larger than the roll, which can range from $-60 \sim 40 \mu\text{rad}$ in this study. So we can safely ignore the roll angle in formula (1) without losing much accuracy and we have:

$$\text{Roll_Torque} \cong \text{Roll_Stiffness} \times \text{RSA} \quad (5)$$

This means that for a given suspension, the roll torque is roughly proportional to RSA. So if we double the RSA, we also double the roll torque. And this is why it is desirable to define roll torque in the current CML static simulator. For a slider design, higher roll torque will increase the slider roll and the resulting roll angle is roughly proportional to the roll torque exerted on the slider. So we have:

$$\text{Roll_Torque} \cong Q \times \text{Roll_Angle} , \quad (6)$$

where Q is a coefficient for a certain air bearing slider. Interestingly, unlike the constant K in formula (3), Q differs from OD to ID for a certain slider design and it is roughly constant for the same disk radial position. This can be verified from the air bearing stiffness matrix given by the CML static simulator Quick4. For example, for the 7nm FH

Pico slider design with 1° PSA and 0° RSA, its pitch torque stiffness coefficients at OD, MD and ID are 0.39, 0.39 and 0.42 (μN-m/μrad), which are quite uniform. But its roll torque stiffness coefficients range from -0.17 to 0.13 (μN-m/μrad) from ID to OD. It is the non-uniformity of the air bearing roll stiffness at different radial positions that causes the different Q value. From Fig. 32 we see that for the smaller size Femto slider, Q is smaller. And from (5) and (6), we have:

$$Roll_Angle \cong \frac{Roll_Stiffness}{Q} \times RSA = Q' \times RSA \quad (7)$$

This is why the roll angle demonstrates a linear relationship with RSA. Since Q' is not a constant at the different disk radial positions for a given slider, the roll rate of change with respect to RSA also differs from OD to ID. For all three slider designs considered in our study, the RSA has larger effects on the roll angle at the OD than at the ID.

Since RSA has greater effects on lower FH slider designs, it causes a very large roll angle changes for the 3.5nm FH Femto slider design, and when the RSA is lower than -0.25° or higher than 0.25°, the resulting large roll angle will crash the Femto slider onto the disk. So we can see that it is critical for the Femto slider design to have a fairly small RSA. Otherwise it will not be able to fly.

Table 4 summarizes the steady flying attitude of the three slider designs with 6.886e-5 (N-m/rad) pitch stiffness and 7.049e-5 (N-m/rad) roll stiffness and 1° PSA and 0° RSA (i.e. the “nominal” case). If we compare Table 4 with Table 3, which shows the simulation results with 0° PSA and 0° RSA, we see that the slider designs have 1 ~ 2 nm

lower FHs, 10 ~ 40 μ rad higher pitch angles when the PSA and RSA effects are taken into account.

4. STIFFNESS EFFECTS ON SLIDER FLYING ATTITUDE

In this section, we investigate the suspension stiffness effects on air bearing slider steady performance with the nominal values of 1° PSA and 0° RSA. We used the 6.886e-5 (N-m/rad) pitch stiffness and 7.049e-5 (N-m/rad) roll stiffness as the original suspension stiffness data. We change the suspension stiffness by factors of the original stiffness data using the factors: 0.1, 0.2, 0.5, 1, 2, 5, 10.

[Figures 33, 34](#) and [35](#) summarize the FH, pitch and roll changes versus stiffness for the three INSIC slider designs, respectively.

We see that, similar to the PSA effects on flying attitude, a higher suspension stiffness causes a lower FH for all three slider designs. And it causes linear increments of the pitch angle. This is reasonable in view of formula (2). When the PSA is fixed, the pitch torque is roughly proportional to pitch stiffness. And by doing analysis similar to those of [Section 3.4](#) we can verify the results of this section. From [Fig. 35](#) we see that like PSA, stiffness does not have large effects on the roll angle compared with FH and pitch angle.

Again we should note that, similar to the PSA, the suspension stiffness has greater effects on lower FH sliders. The 7nm and 5nm FH INSIC Pico sliders can fly with a suspension stiffness 5 times higher than the original one. But the 3.5nm FH INSIC Femto slider can no longer fly if we double the suspension stiffness. Therefore, lower FH slider designs have stricter constraints on suspension stiffness.

5. *CONCLUSION*

In this report, we investigated the PSA and RSA effects on the steady performance of three INSIC slider designs.

We found that larger PSA causes lower FH and higher pitch. And the changes of FH and pitch show a linear trend of change with respect to PSA change. The PSA does not have large effects on roll when the RSA is fixed. We also found that the PSA has greater effects on slider designs of smaller size and lower FH.

Our simulation results show that a larger RSA causes higher roll. Roll shows a linear trend of change with respect to RSA change. RSA effects on FH are not linear and depend on the slider air bearing surface shape and the location of the transducer. RSA has little effect on pitch, and lower FH slider designs are more sensitive to RSA. RSA values should be kept as small as possible.

We also explored the suspension stiffness effects on slider steady performance with 1° PSA and 0° RSA. We found that suspension stiffness demonstrates similar effects as PSA does on slider steady performance.

From the above investigations, we would like to make the following points:

1. PSA, RSA and suspension stiffness have larger effects on lower FH slider designs. Instead of assuming 0 pitch torque and 0 roll torque, we must take all of them into account when designing ultra-low FH sliders.
2. Depending on different Head-Suspension-Assemblies, the pitch torque usually ranges from $0.5 \sim 1.5$ ($\mu\text{N}\cdot\text{m}$) and roll torque usually takes the value 0.
3. Air bearing slider designs will have different steady performance when they are mounted to different suspensions. Stiffer suspension will result in a larger pitch angle and low FH with nominal 1° PSA and 0° RSA.
4. Air bearing slider designs even have different flying attitudes with the same suspension when the PSA and RSA are different. Larger PSA will result in lower FH and higher pitch angles. And larger RSA will result in higher roll angles.
5. With zero suspension roll torque, if we do not consider the intermolecular force effects and there is no contact, the roll moment will be balanced by the moments of the shear force and the air bearing force.

6. Since PSA and RSA have large effects on slider steady performance, they are expected to also have large effects on slider dynamic performance.

ACKNOWLEDGEMENT

This study is supported by the Computer Mechanics Laboratory (CML) at the University of California at Berkeley and partially supported by the Extremely High Density Recordings (EHDR) project of the Information Storage Industry Consortium (INSIC).

REFERENCES

1. Zeng, Q.-H. and Bogy, D., 1999, “The CML Dynamic Load/Unload Simulator (Version 421.40)”, Technical Report 99-005, Computer Mechanics Laboratory, University of California at Berkeley.
2. Lu, S. and Bogy, D., 1997, “Numerical Simulation of Slider Air Bearings”, Doctoral Dissertation No. 97-004, Computer Mechanics Laboratory, University of California at Berkeley.
3. Hu, Y. and Bogy, D., 1996, “Head-Disk-Suspension Dynamics”, Doctoral Dissertation No. 96-001, Computer Mechanics Laboratory, University of California at Berkeley.
4. Grisso, R., Lu, S. and Bogy, D., 1997, “CML Air Bearing Design Program (Version 4.0.17) and 32-bit Windows Interface”, Technical Report 97-013, Computer Mechanics Laboratory, University of California at Berkeley.
5. Chen, L., Hu, Y. and Bogy, D., 1997, “The CML Air Bearing Dynamic Simulator Version 4.21”, Technical Report 97-018, Computer Mechanics Laboratory, University of California at Berkeley.

	7nm FH Pico	5nm FH Pico	3.5nm FH Femto
Slider Length (mm)	1.25	1.25	0.85
Slider Width (mm)	1	1	0.7
Slider Height (mm)	0.3	0.3	0.23
Crown (nm)	25.4	25.4	18
Camber (nm)	2.5	2.5	2.5
Twist (nm)	0	0	0
Preload (g)	1.5	1.5	0.8
P Offset (um)	0	0	0
R Offset (um)	0	0	0
Pitch Stiffness (N-m/rad)	6.886e-5	6.886e-5	6.886e-5
Roll Stiffness (N-m/rad)	7.049e-5	7.049e-5	7.049e-5
RPM	7200	7200	10000
OD, MD, ID (mm)	31, 23, 15	31, 23, 15	22.9, 17.1, 11.4
Skew Angles (degree)	17.39, 9.1, -1.22	17.39, 9.1, -1.22	6.65, 1.1, -6.65

Table 1 Summary of slider and suspension parameters used by modified static simulator

	7nm FH Pico			5nm FH Pico			3.5nm FH Femto		
	OD	MD	ID	OD	MD	ID	OD	MD	ID
FH (nm)	6.92	7.10	6.91	5.13	4.75	5.15	3.51	2.09	3.54
Pitch (μrad)	207.6	167.0	116.1	264.7	220.5	162.0	243.6	206.1	156.7
Roll (μrad)	-4.53	-1.56	-2.62	0.84	0.43	-3.11	-0.06	1.15	2.32

Table 2 Flying attitude of air bearing sliders with 0 pitch stiffness and 0 roll stiffness

	7nm FH Pico			5nm FH Pico			3.5nm FH Femto		
	OD	MD	ID	OD	MD	ID	OD	MD	ID
FH (nm)	6.81	7.06	6.89	5.14	4.78	5.17	3.54	2.11	3.55
Pitch (μrad)	207.5	167.1	116.1	264.4	220.3	161.8	243.1	205.7	156.4
Roll (μrad)	-4.47	-1.49	-2.19	0.86	0.45	-3.07	0.01	1.16	2.28

Table 3 Flying attitude of air bearing sliders with $6.886e-5$ (N-m/rad) pitch stiffness and $7.049e-5$ (N-m/rad) roll stiffness and 0° PSA and 0° RSA

	7nm FH Pico			5nm FH Pico			3.5nm FH Femto		
	OD	MD	ID	OD	MD	ID	OD	MD	ID
FH (nm)	5.78	5.80	5.73	4.13	3.59	3.85	1.29	0.40	1.53
Pitch (μrad)	221.3	179.2	126.3	281.7	235.3	174.8	281.3	238.1	187.2
Roll (μrad)	-4.21	-1.31	-2.09	0.84	0.39	-3.09	-1.08	1.60	3.85

Table 4 Flying attitude of air bearing sliders with $6.886e-5$ (N-m/rad) pitch stiffness and $7.049e-5$ (N-m/rad) roll stiffness and 1° PSA and 0° RSA

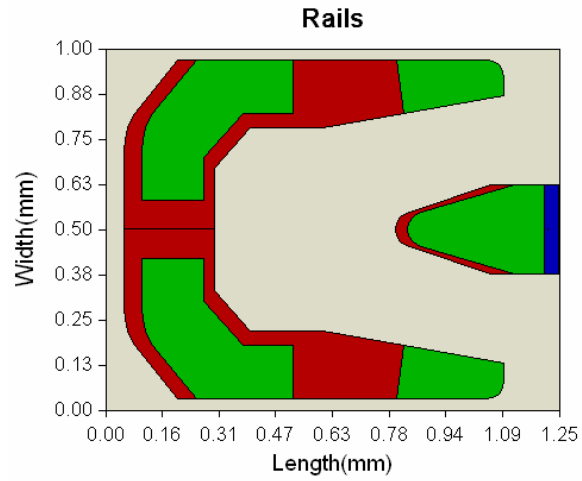


Fig. 1 Rail shape of 7nm FH INSIC Pico slider

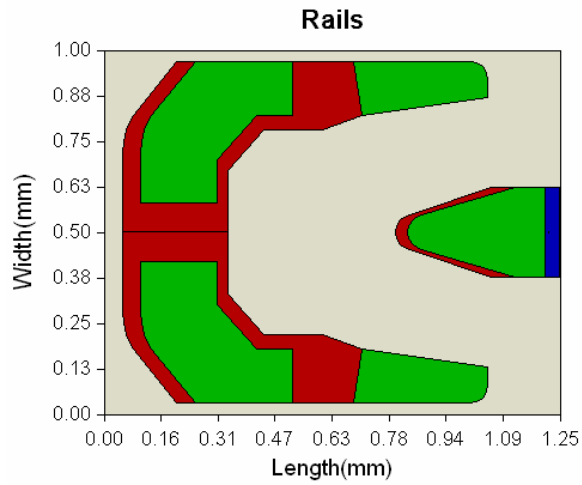


Fig. 2 Rail shape of 5nm FH INSIC Pico slider

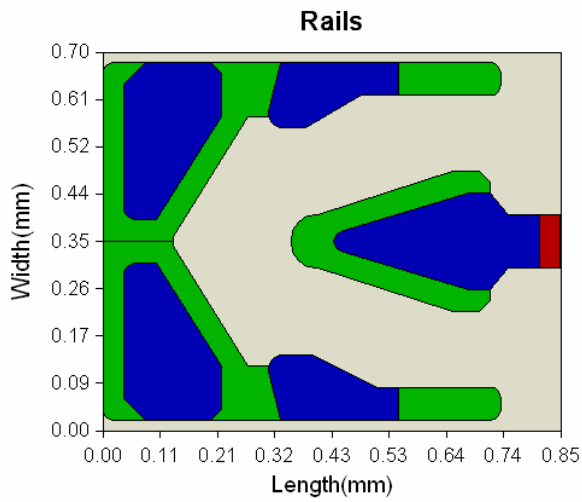


Fig. 3 Rail shape of 3.5nm FH INSIC Femto slider

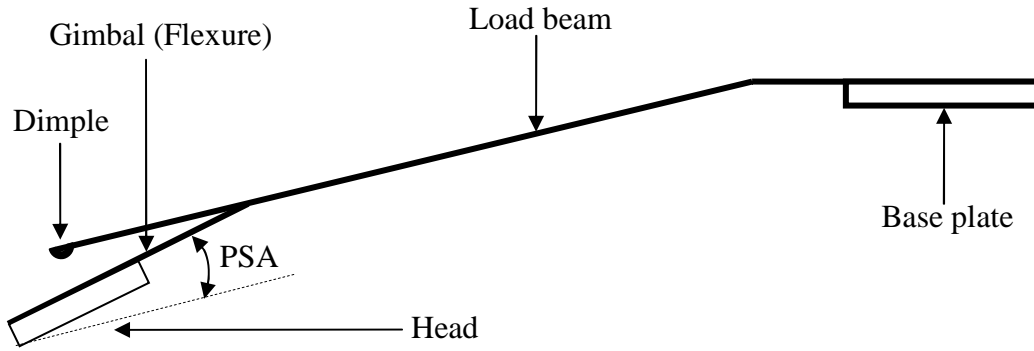


Fig. 4 Typical suspension at unloaded state with positive PSA

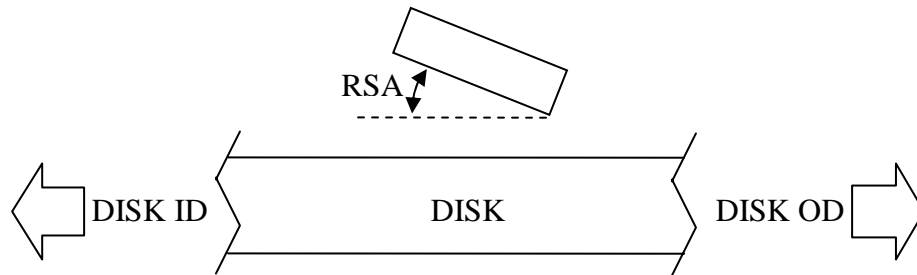


Fig. 5 Definition of positive RSA at unloaded state



Fig. 6 Typical suspension at loaded state

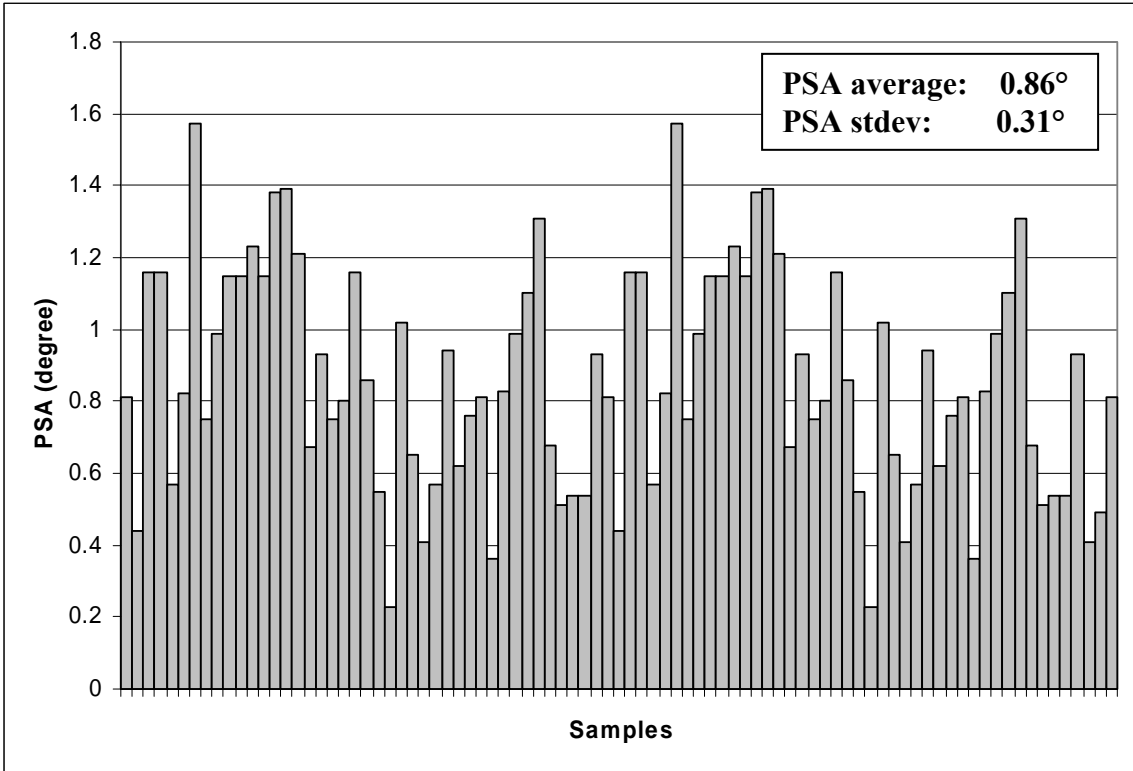


Fig. 7 PSA data for different 7nm FH INSIC Pico slider samples (by Seagate)

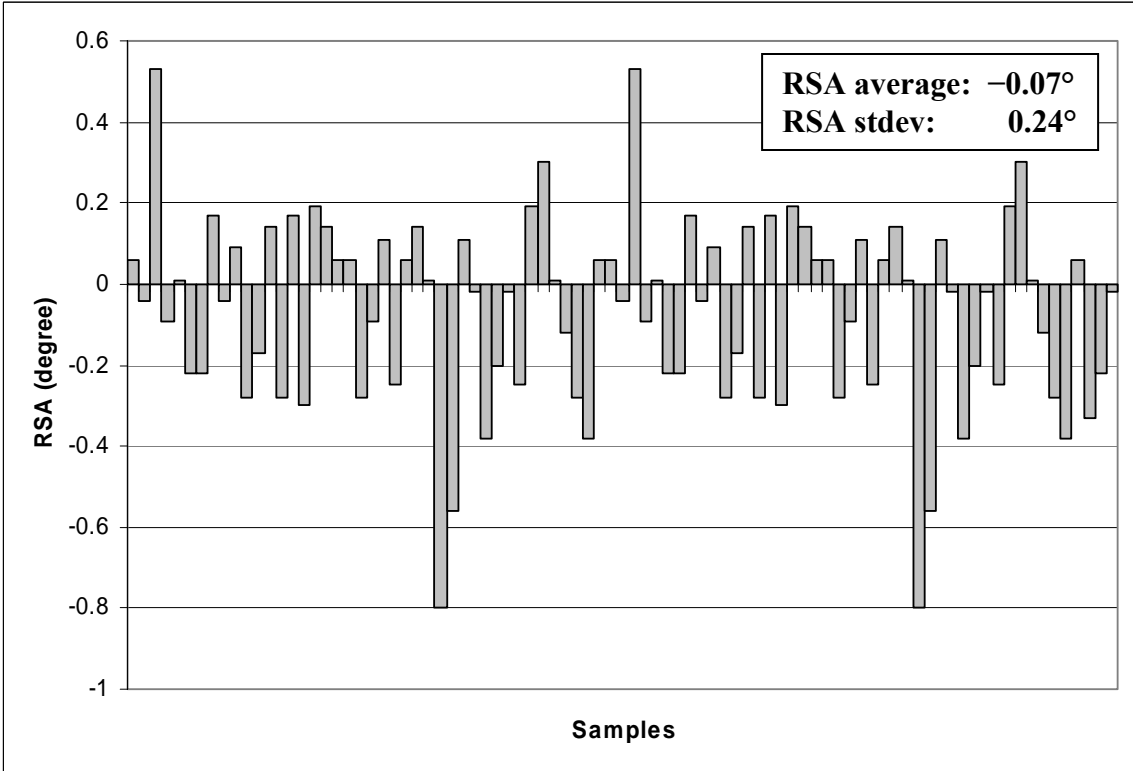


Fig. 8 RSA data for different 7nm FH INSIC Pico slider samples (by Seagate)

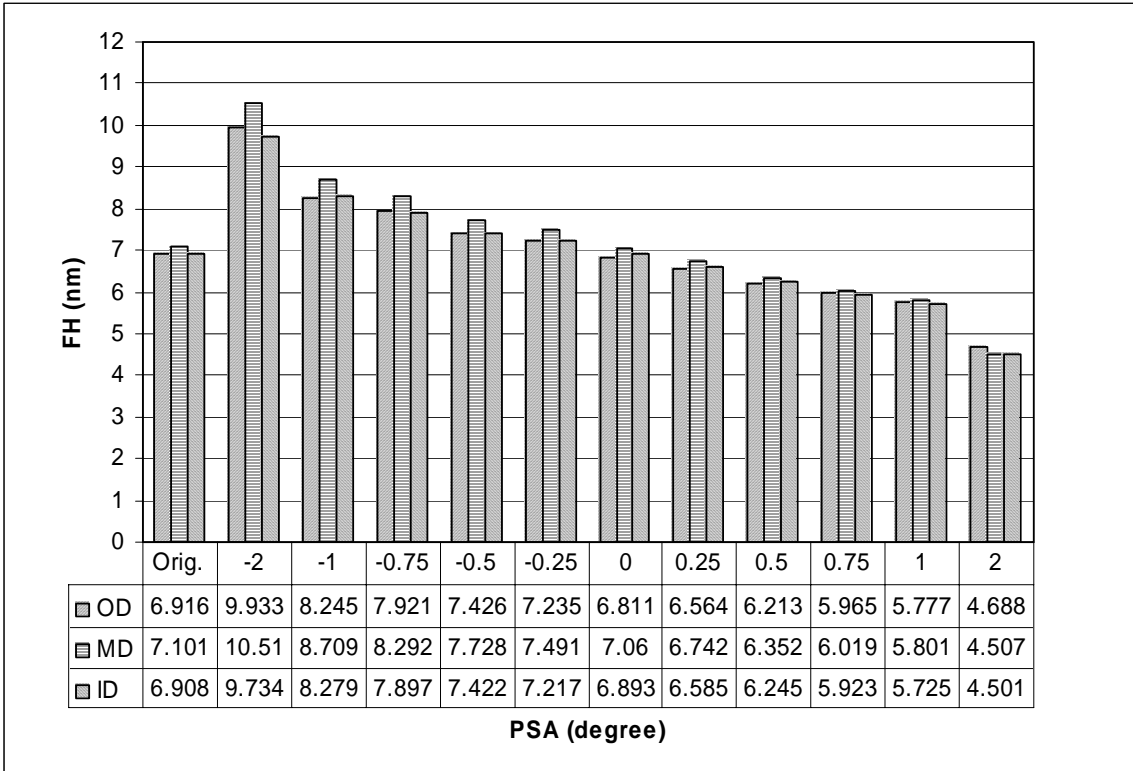


Fig. 9 FH versus PSA (RSA = 0°) for 7nm FH INSIC Pico slider

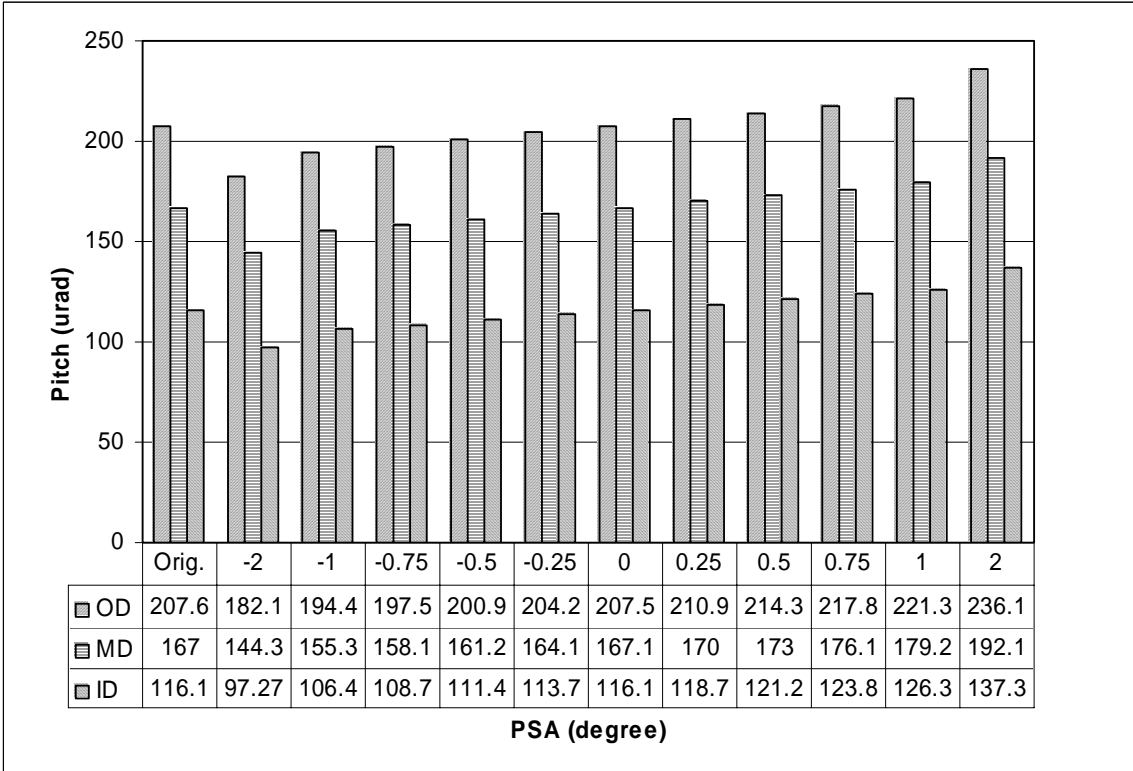


Fig. 10 Pitch versus PSA (RSA = 0°) for 7nm FH INSIC Pico slider

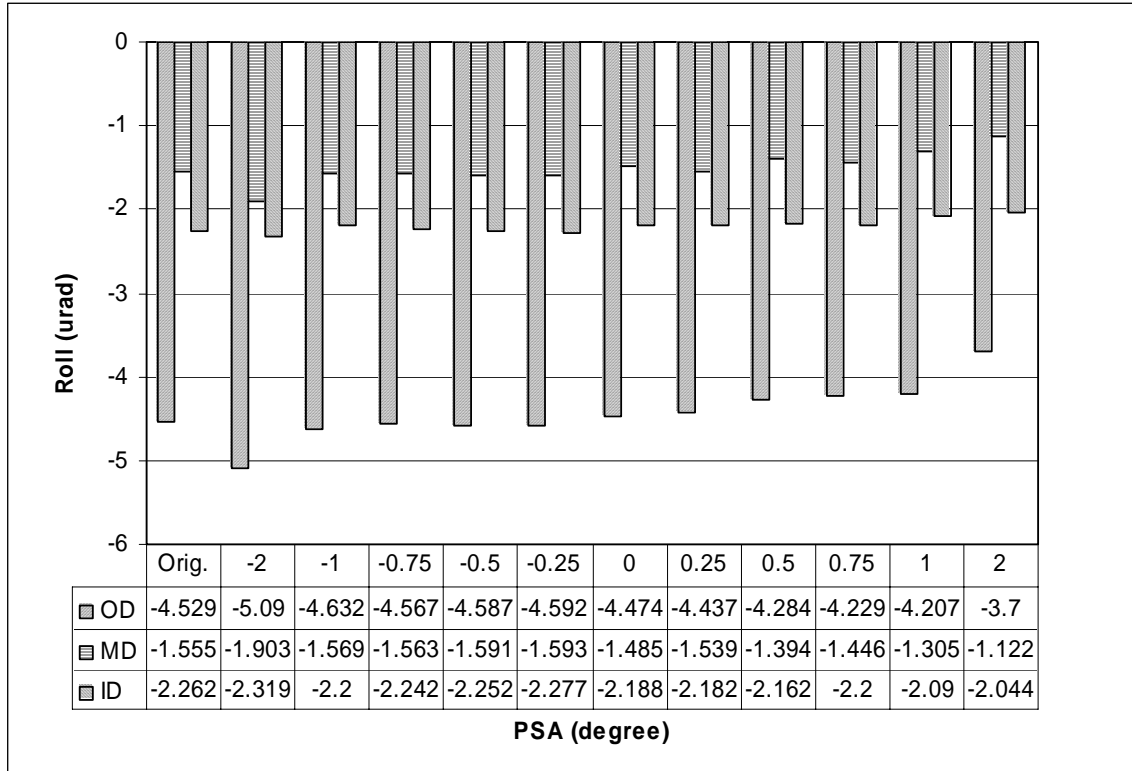


Fig. 11 Roll versus PSA (RSA = 0°) for 7nm FH INSIC Pico slider

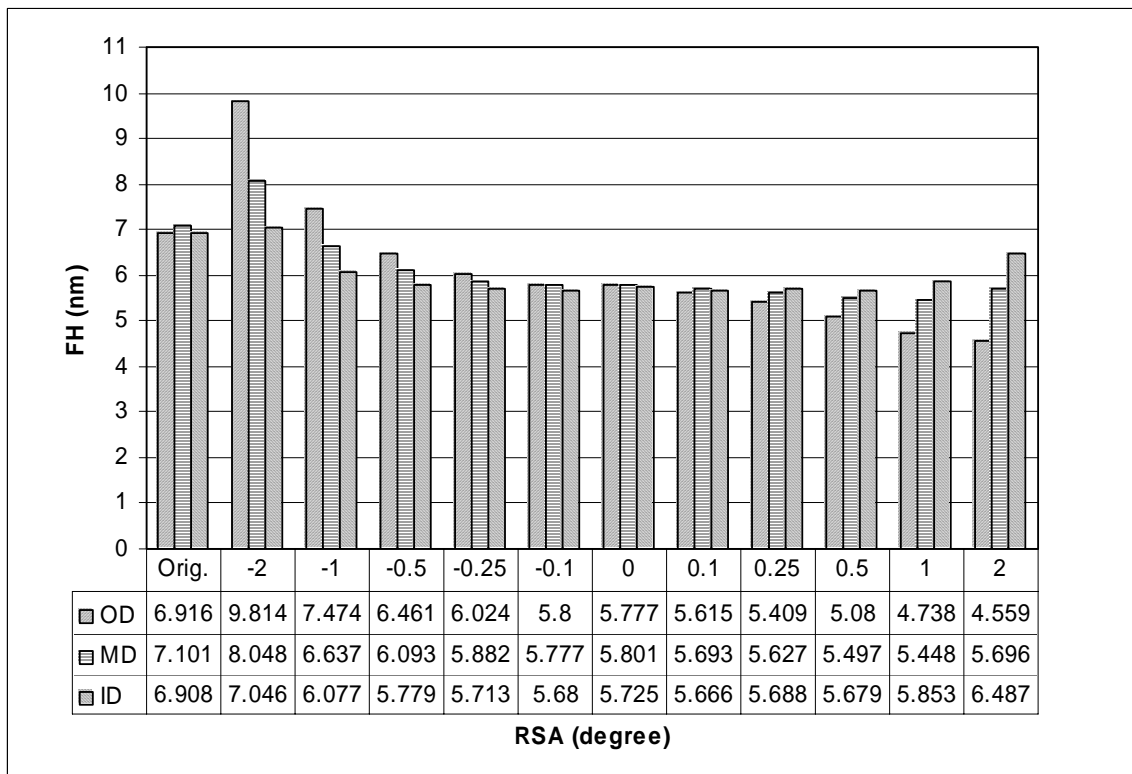


Fig. 12 FH versus RSA (PSA = 1°) for 7nm FH INSIC Pico slider

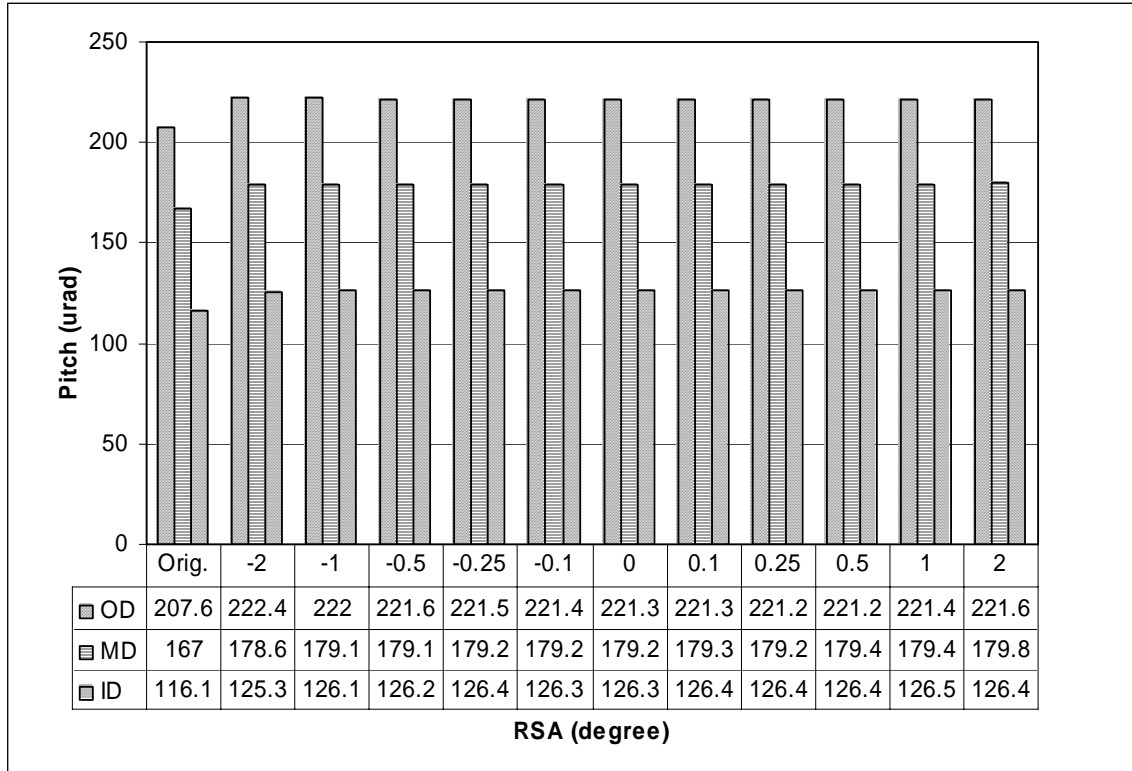


Fig. 13 Pitch versus RSA (PSA = 1°) for 7nm FH INSIC Pico slider

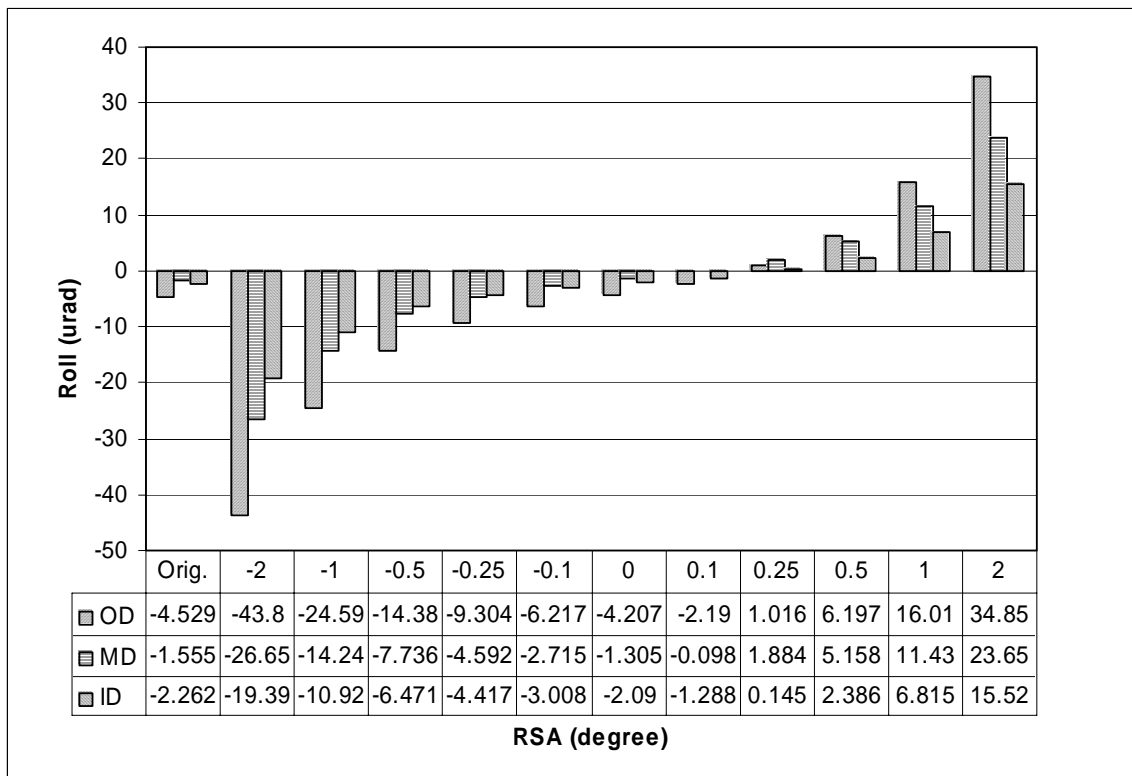


Fig. 14 Roll versus RSA (PSA = 1°) for 7nm FH INSIC Pico slider

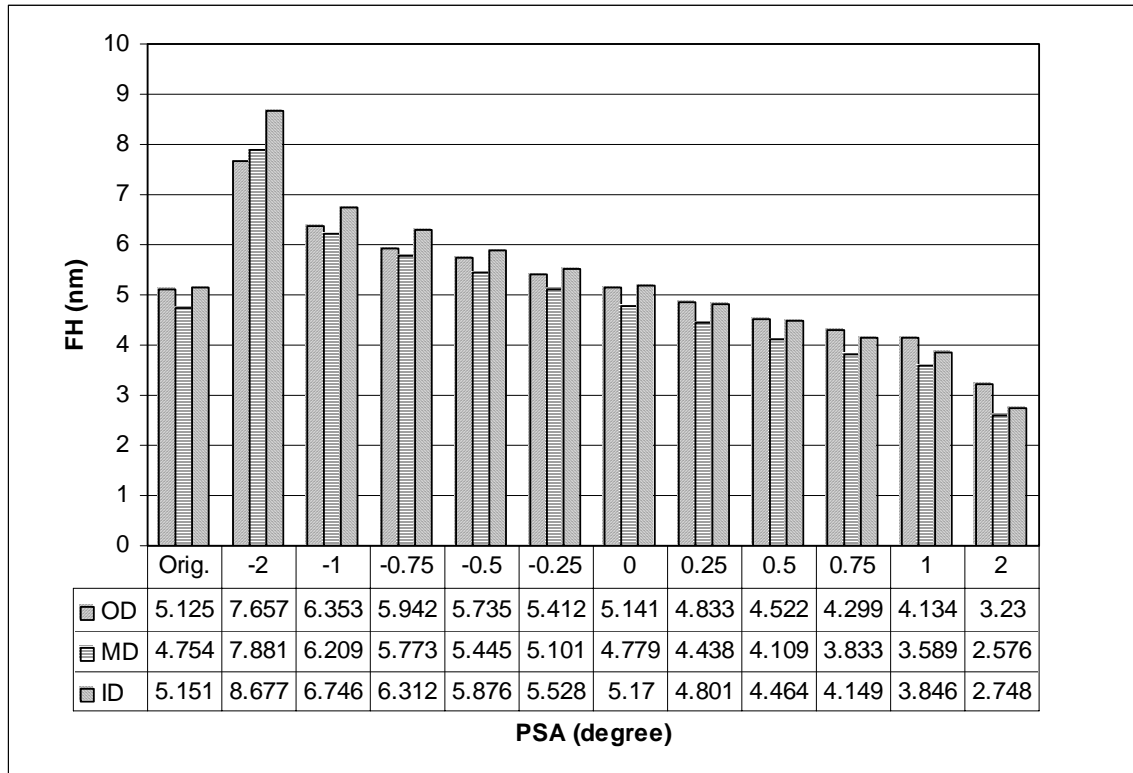


Fig. 15 FH versus PSA (RSA = 0°) for 5nm FH INSIC Pico slider

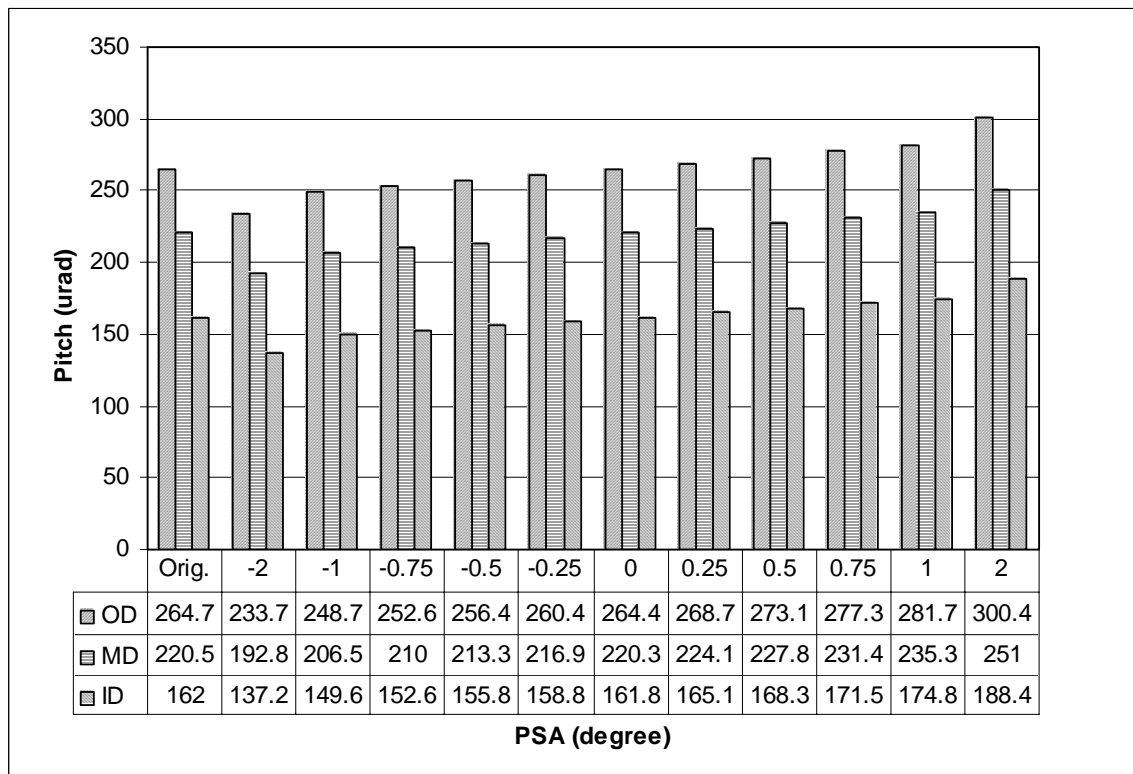


Fig. 16 Pitch versus PSA (RSA = 0°) for 5nm FH INSIC Pico slider

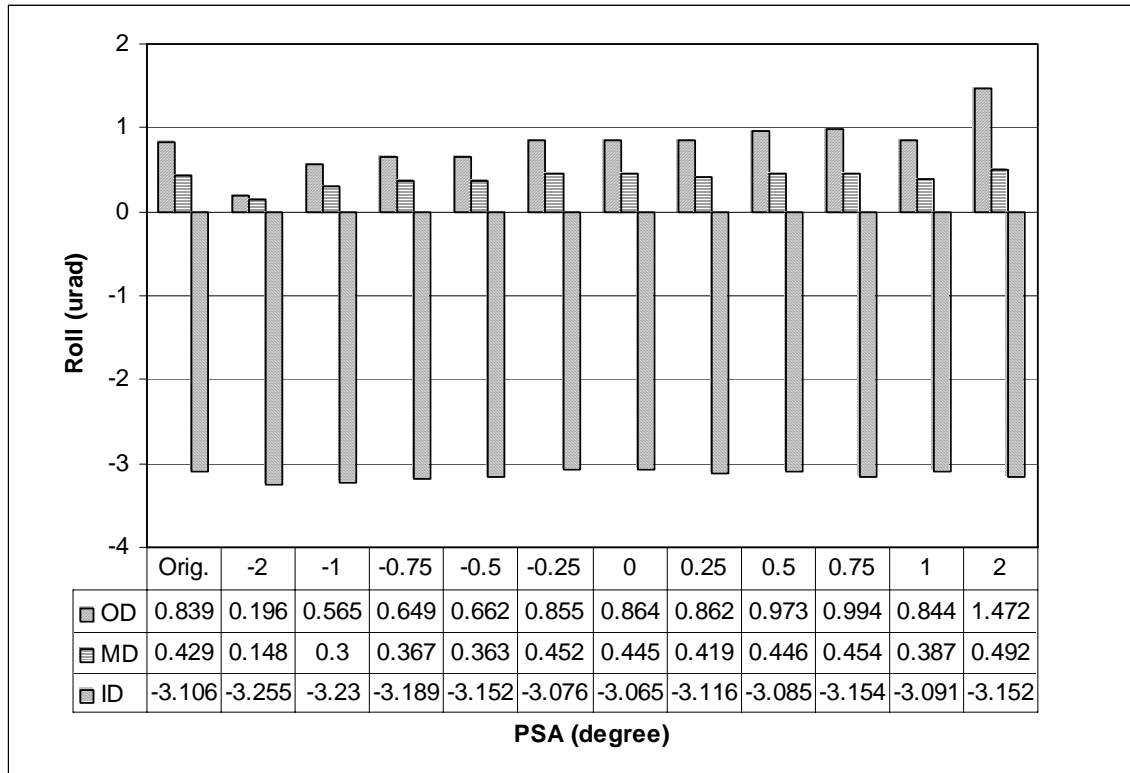


Fig. 17 Roll versus PSA (RSA = 0°) for 5nm FH INSIC Pico slider

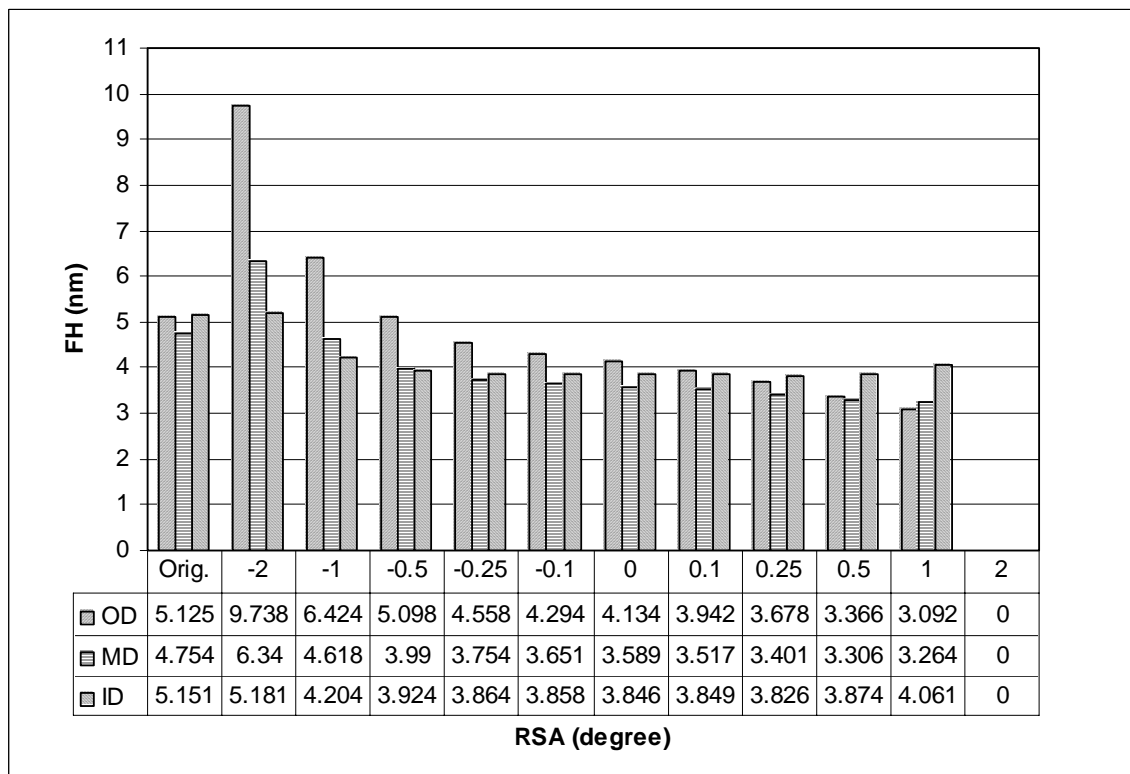


Fig. 18 FH versus RSA (PSA = 1°) for 5nm FH INSIC Pico slider

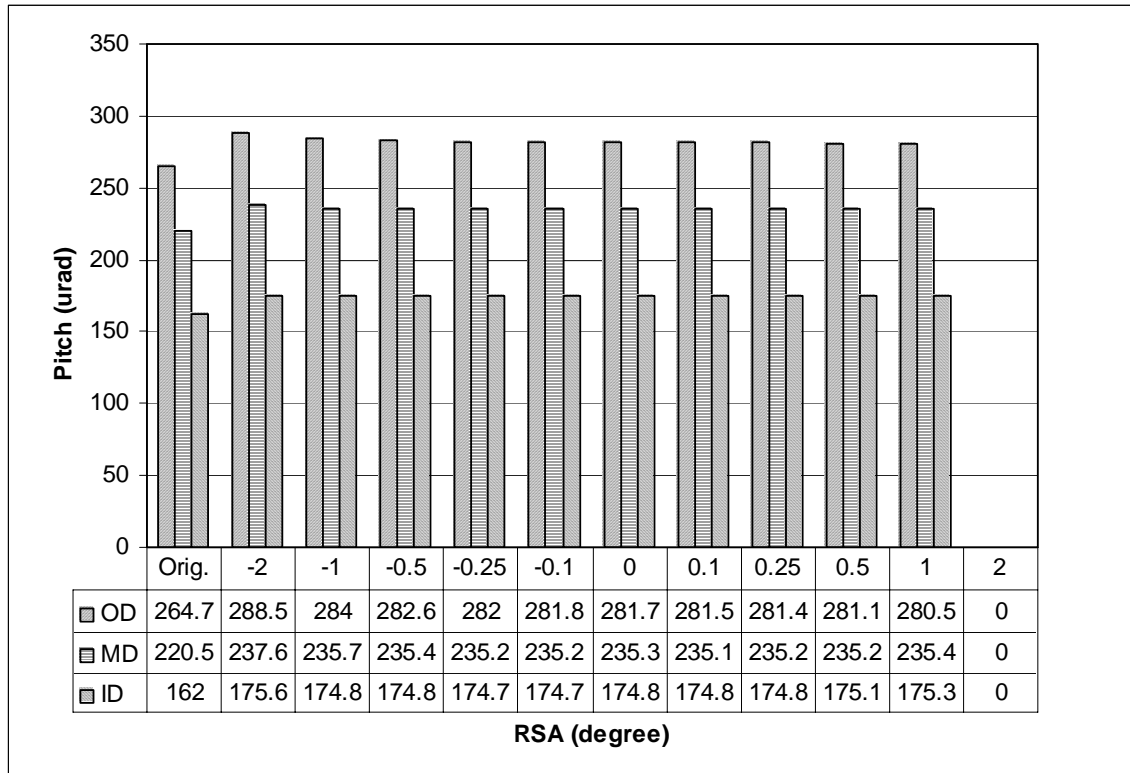


Fig. 19 Pitch versus RSA (PSA = 1°) for 5nm FH INSIC Pico slider

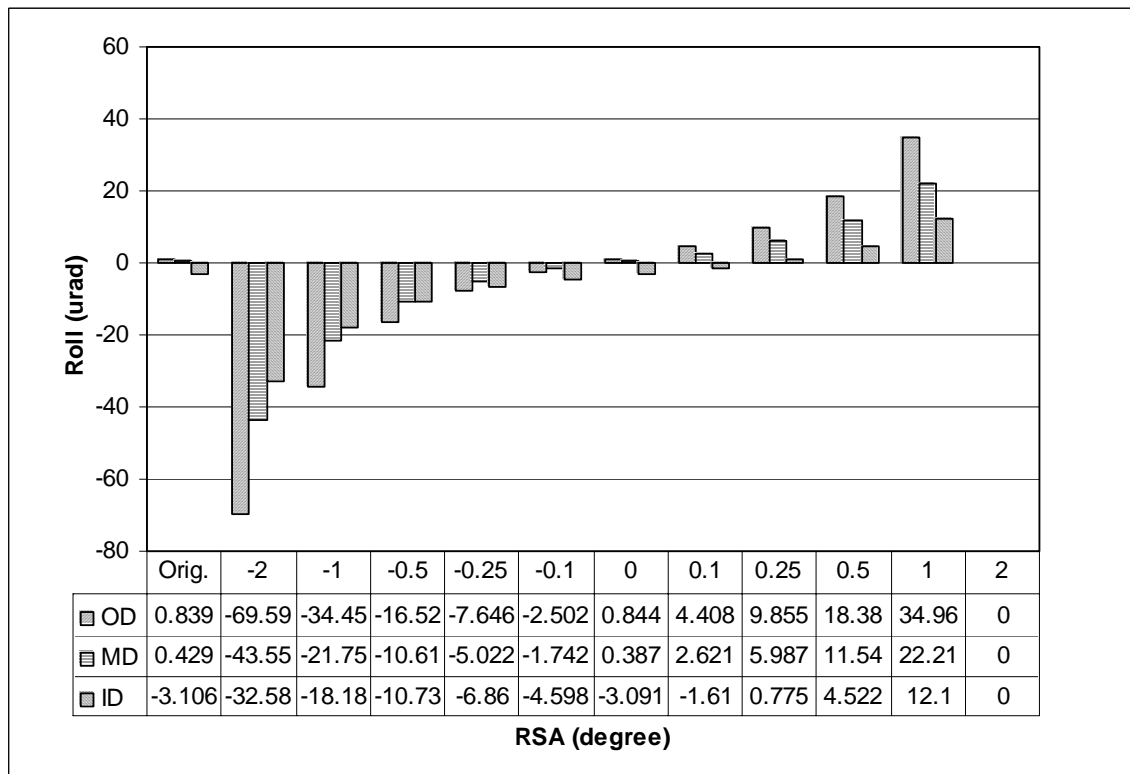


Fig. 20 Roll versus RSA (PSA = 1°) for 5nm FH INSIC Pico slider

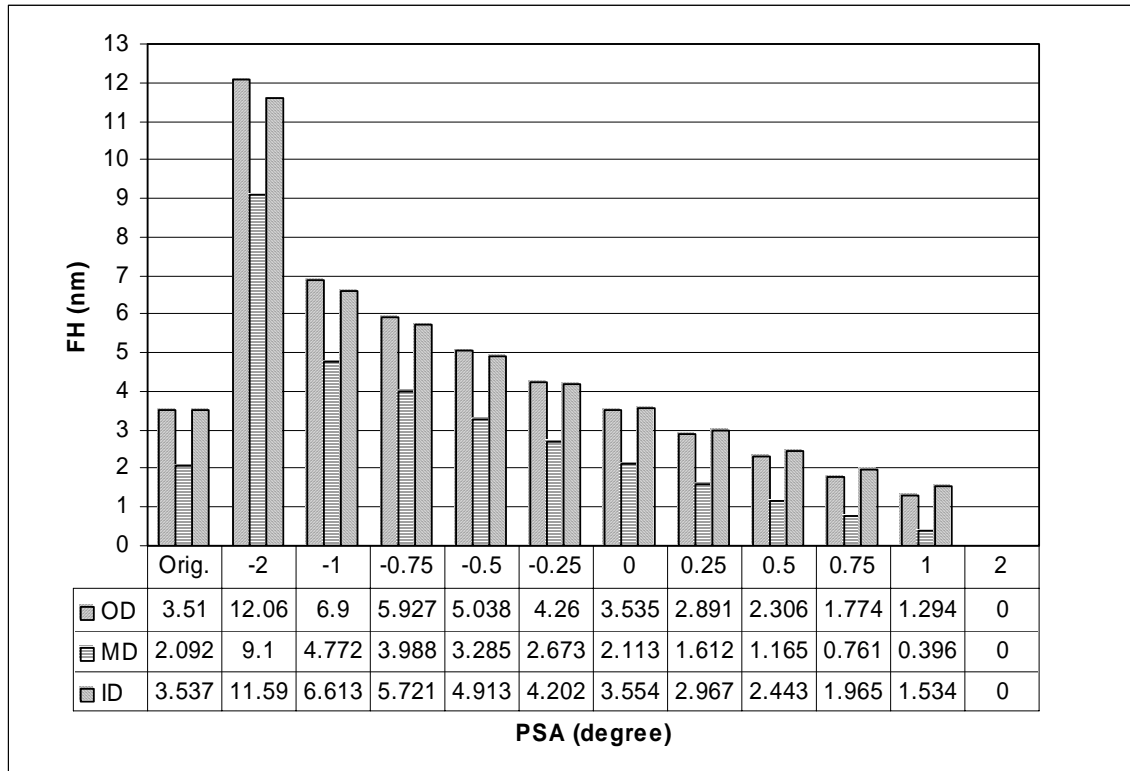


Fig. 21 FH versus PSA (RSA = 0°) for 3.5nm FH INSIC Femto slider

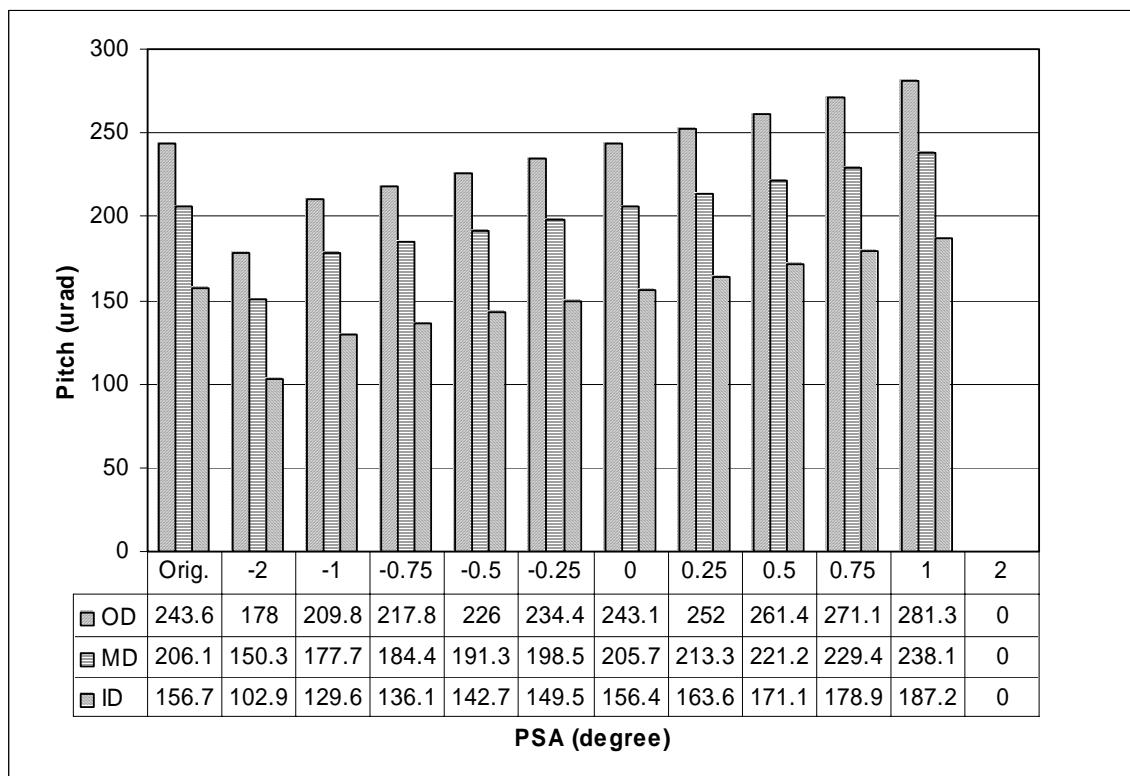


Fig. 22 Pitch versus PSA (RSA = 0°) for 3.5nm FH INSIC Femto slider

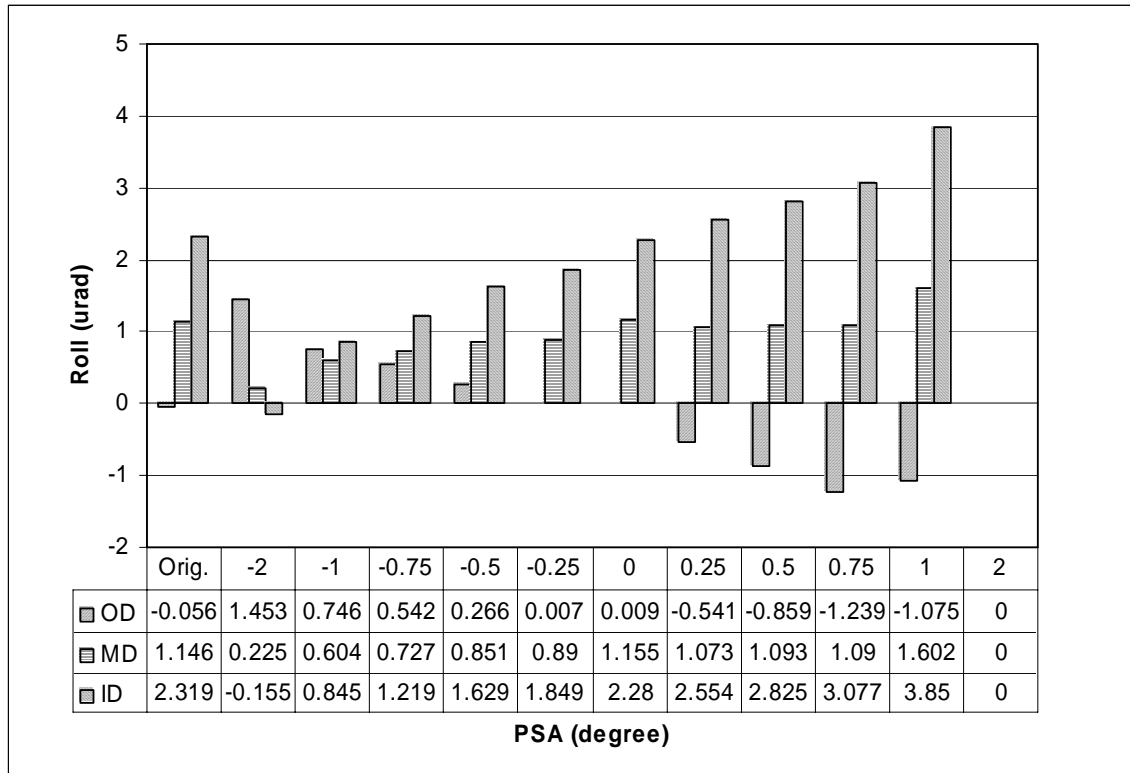


Fig. 23 Roll versus PSA (RSA = 0°) for 3.5nm FH INSIC Femto slider

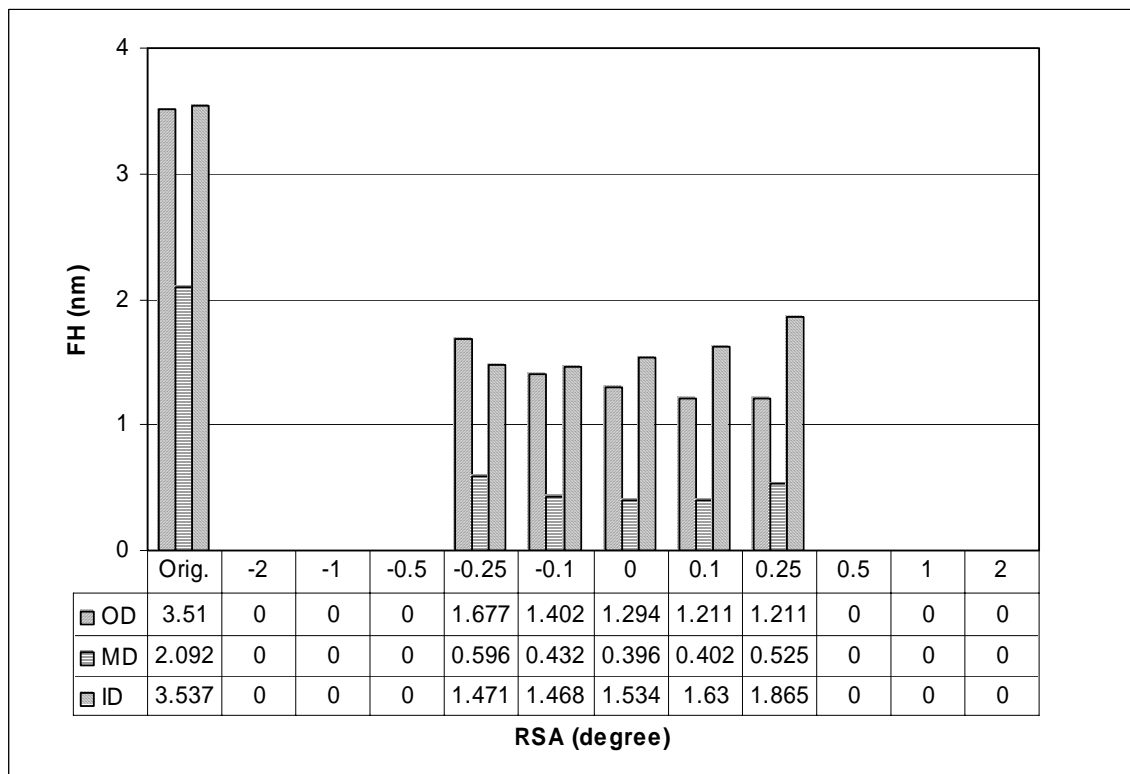


Fig. 24 FH versus RSA (PSA = 1°) for 3.5nm FH INSIC Femto slider

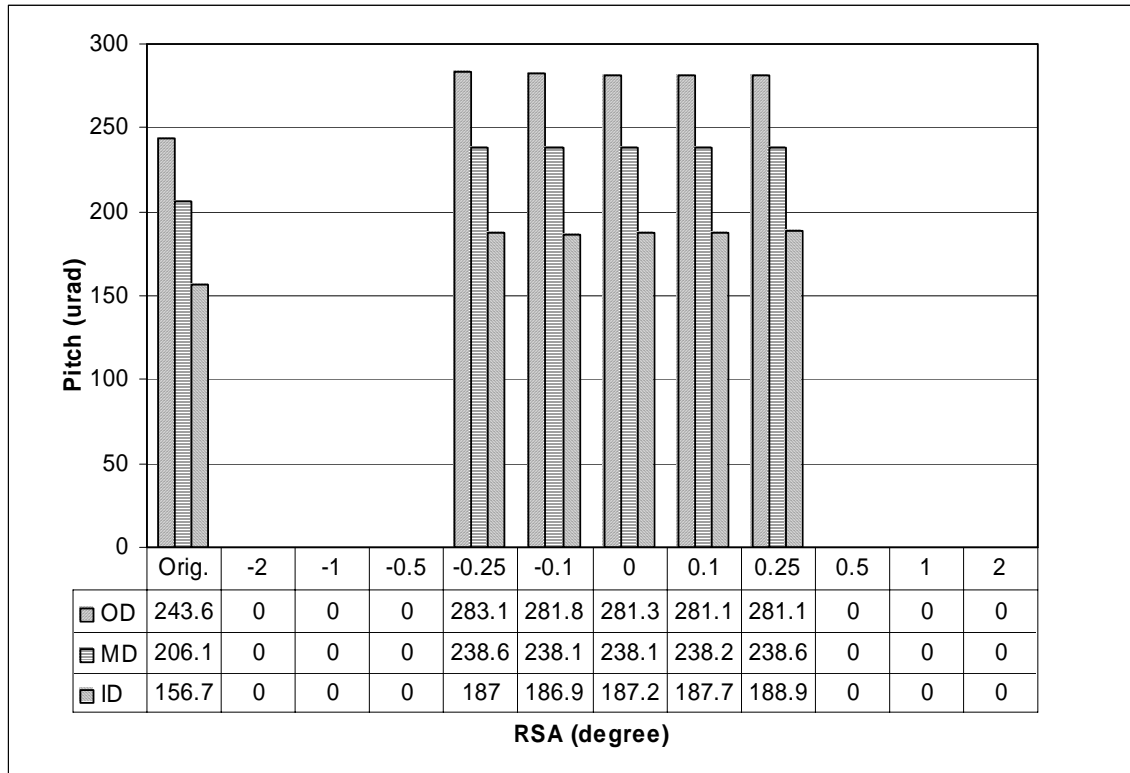


Fig. 25 Pitch versus RSA (PSA = 1°) for 3.5nm FH INSIC Femto slider

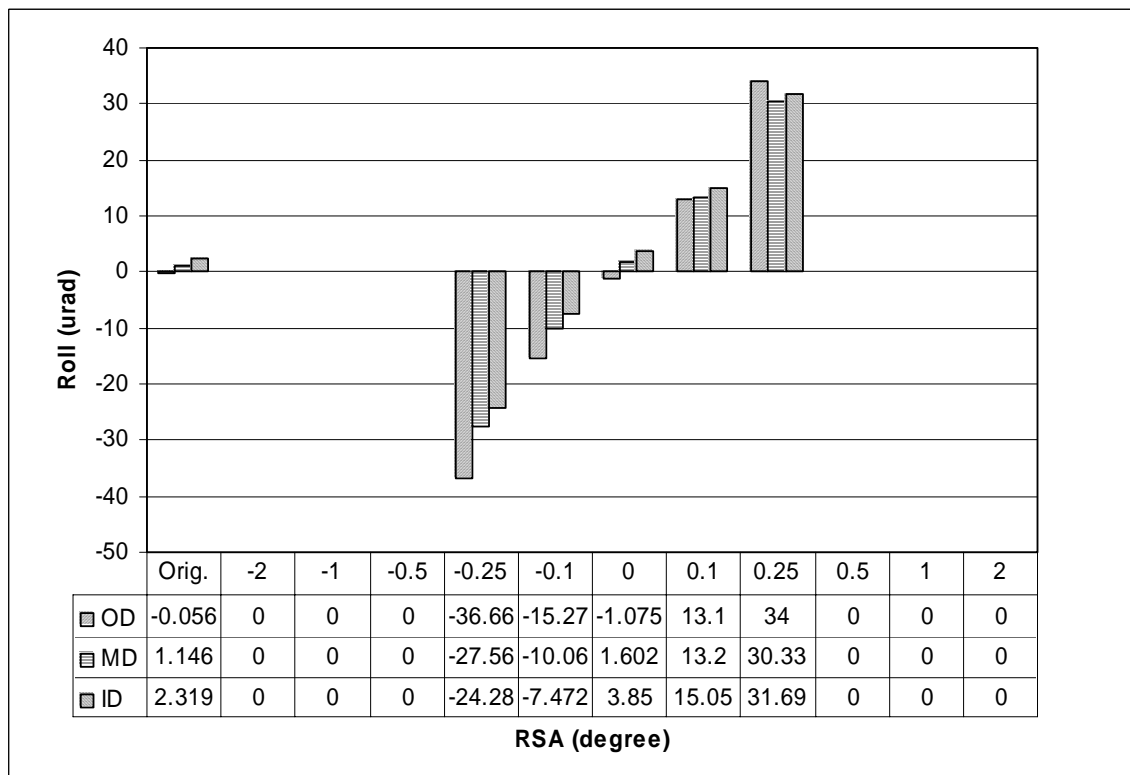


Fig. 26 Roll versus RSA (PSA = 1°) for 3.5nm FH INSIC Femto slider

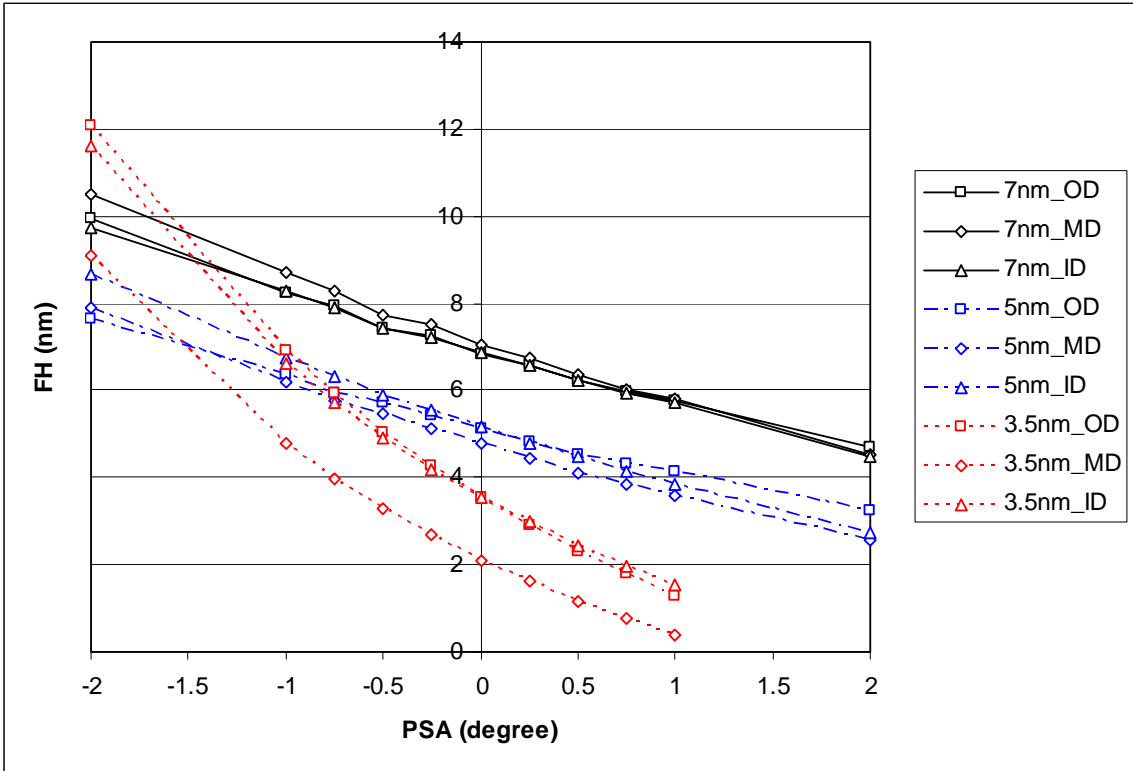


Fig. 27 FH versus PSA (RSA = 0°) for three different slider designs

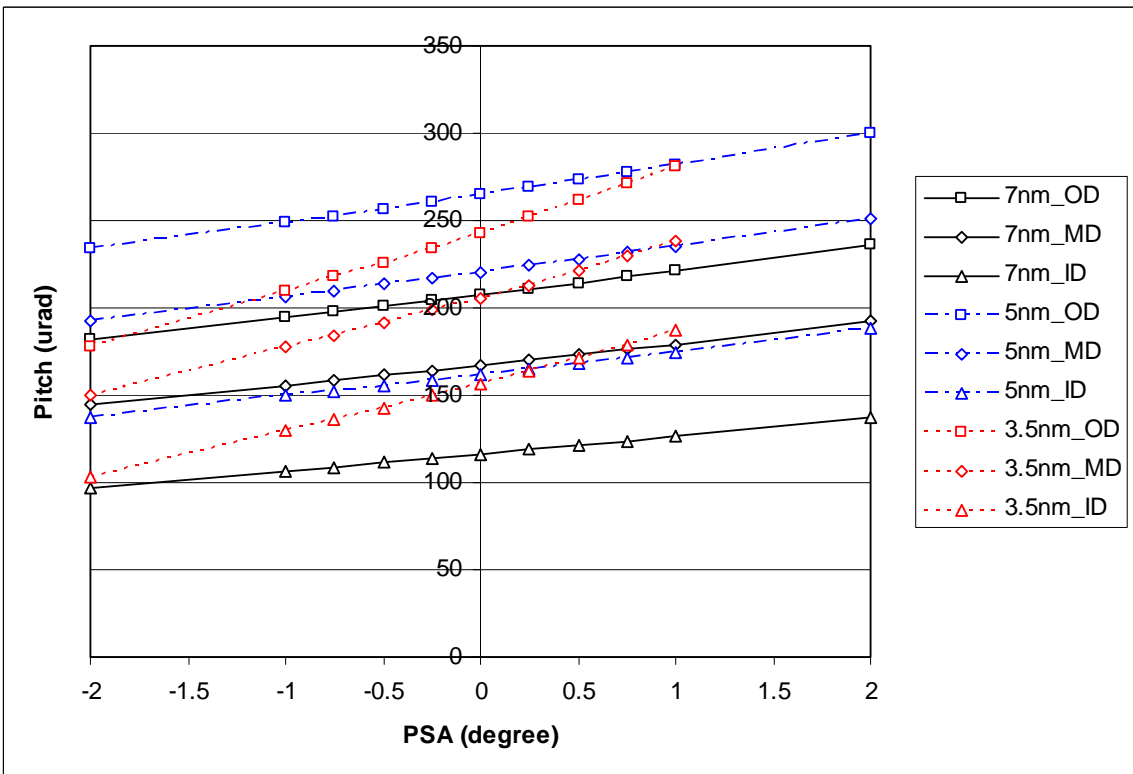


Fig. 28 Pitch versus PSA (RSA = 0°) for three different slider designs

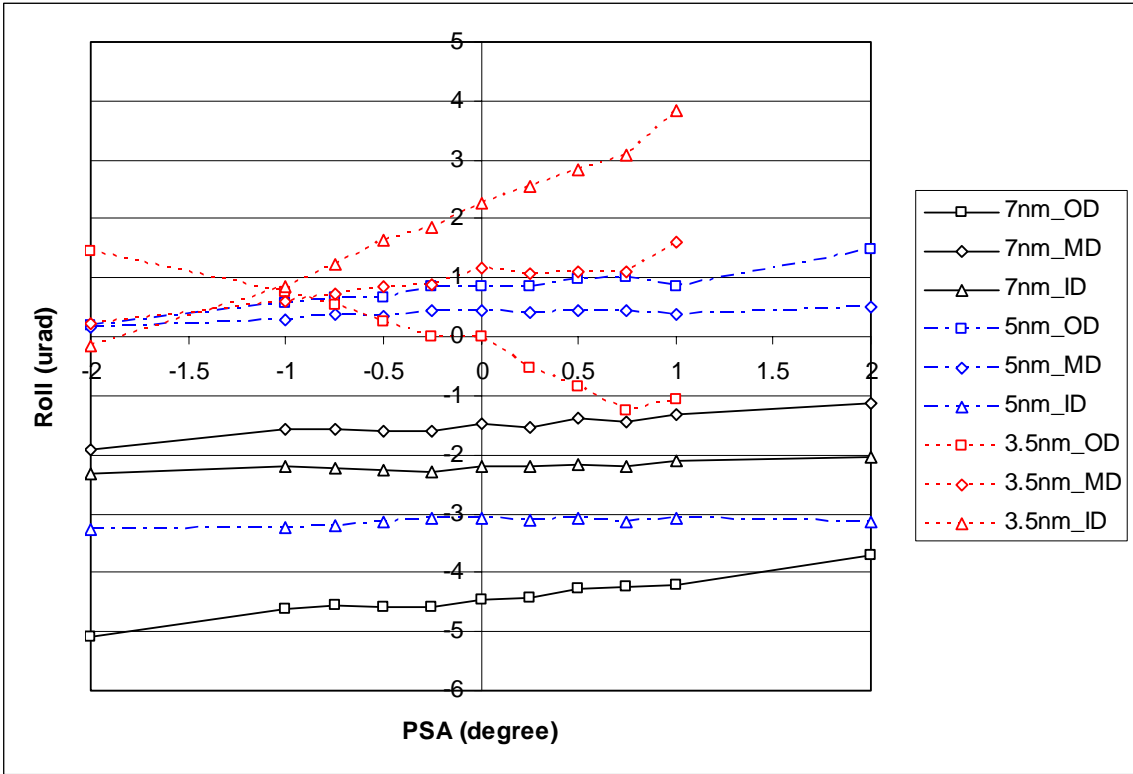


Fig. 29 Roll versus PSA (RSA = 0°) for three different slider designs

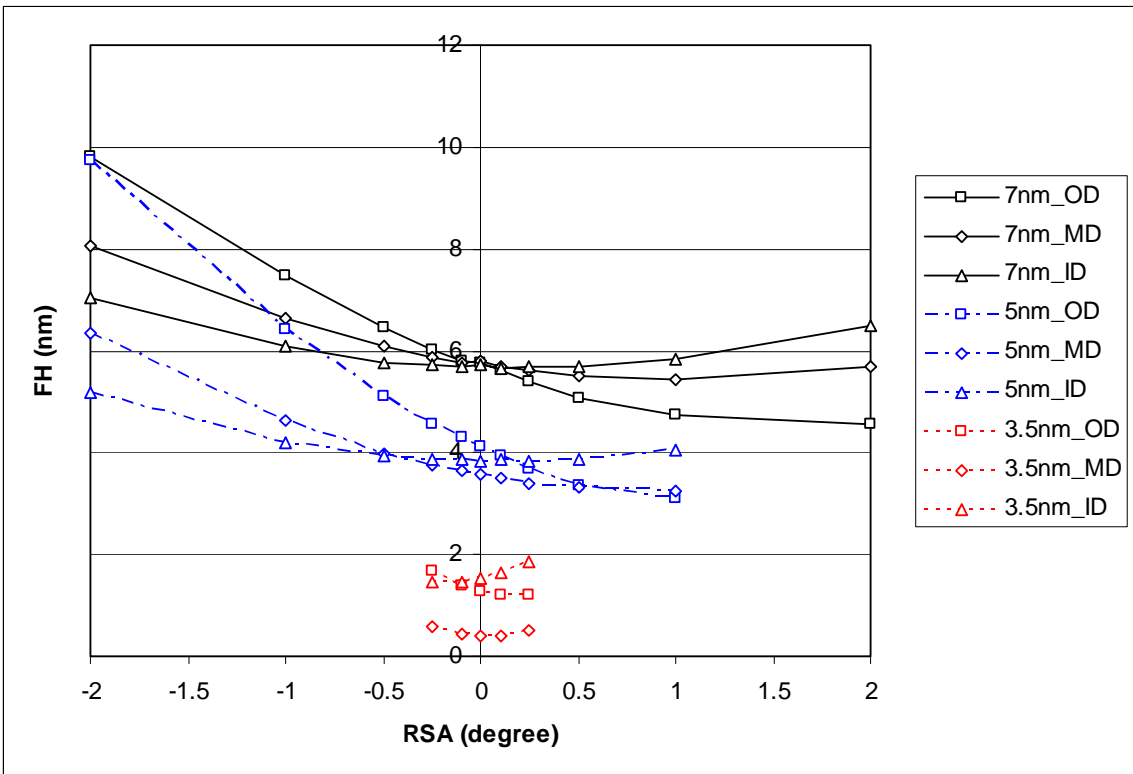


Fig. 30 FH versus RSA (PSA = 1°) for three different slider designs

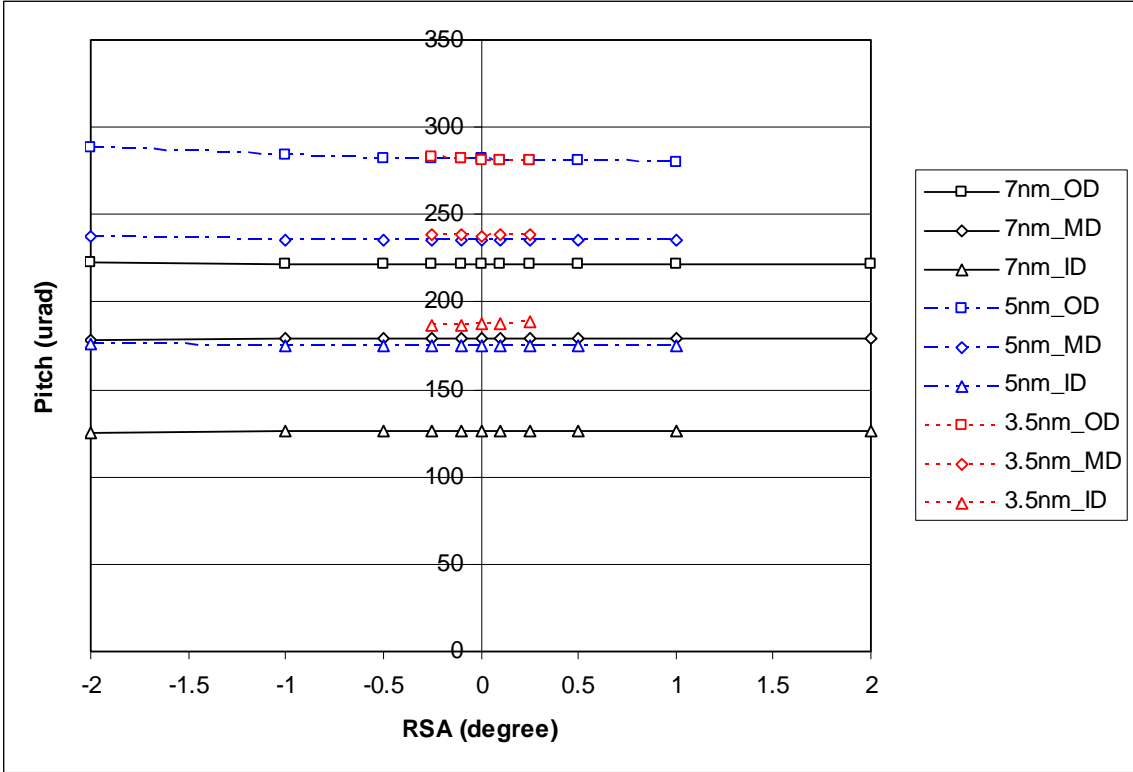


Fig. 31 Pitch versus RSA (PSA = 1°) for three different slider designs

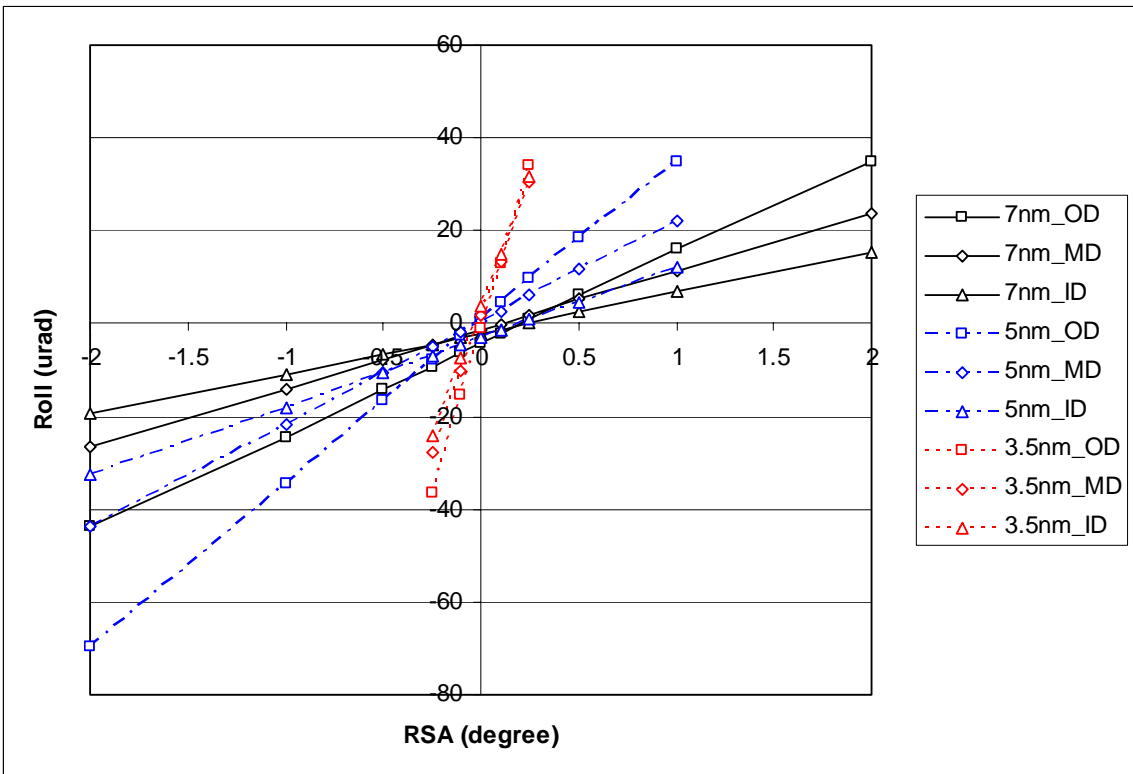


Fig. 32 Roll versus RSA (PSA = 1°) for three different slider designs

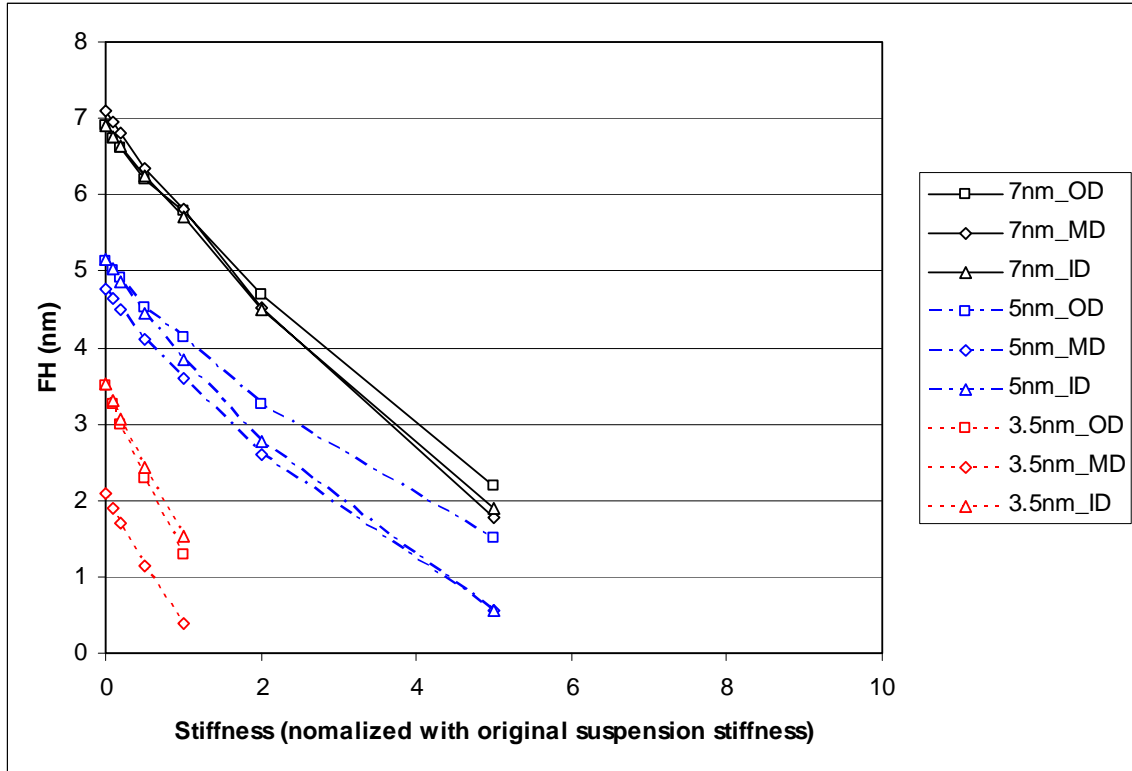


Fig. 33 FH versus stiffness (with 1° PSA and 0° RSA) for three different slider designs

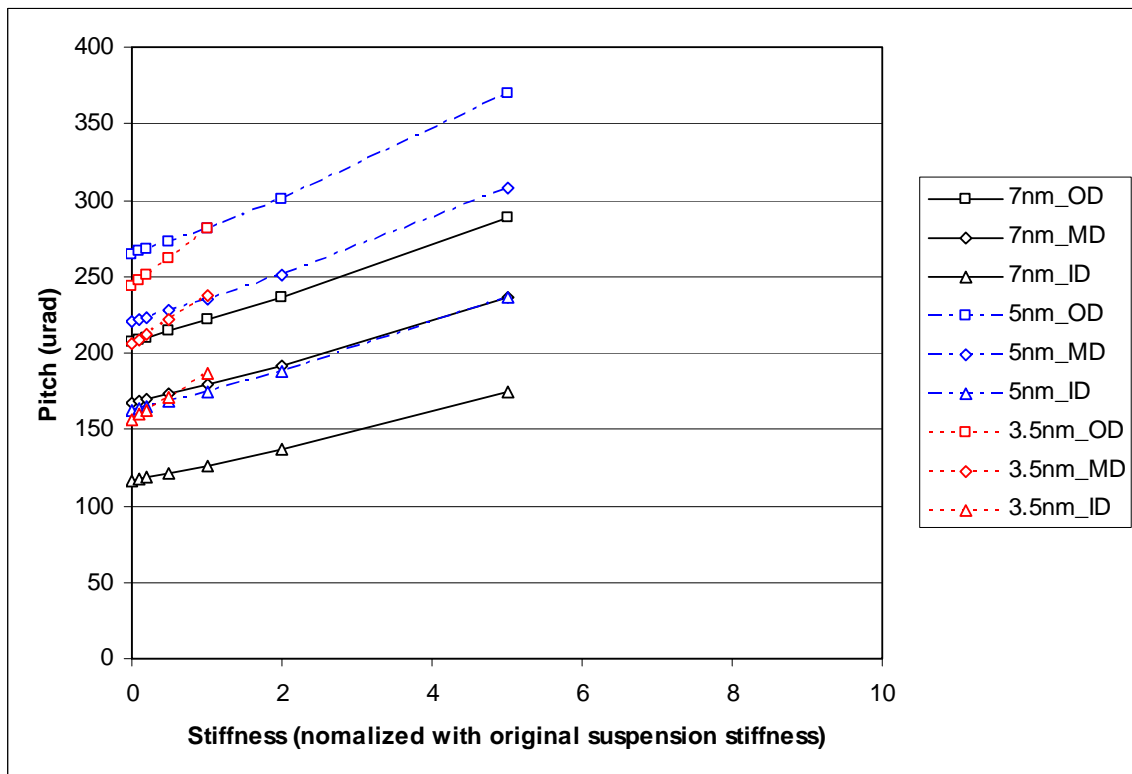


Fig. 34 Pitch versus stiffness (with 1° PSA and 0° RSA) for three different slider designs

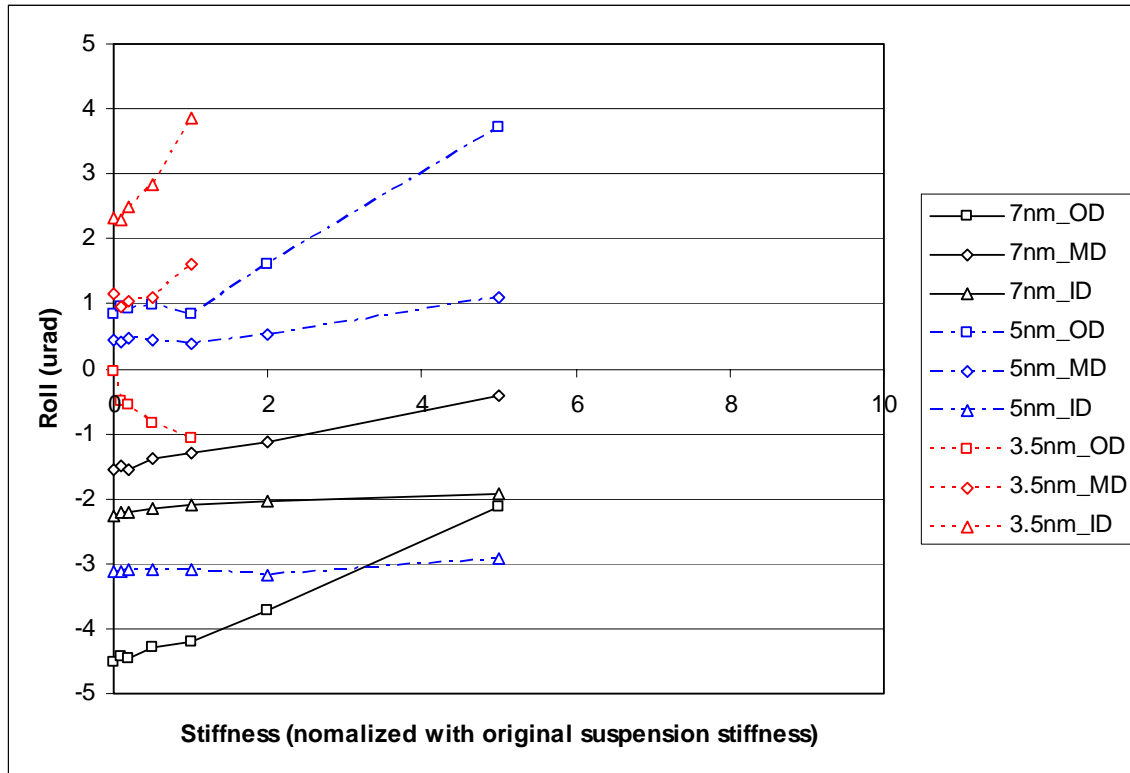


Fig. 35 Roll versus stiffness (with 1° PSA and 0° RSA) for three different slider designs